Sedimentary Processes Influencing Divergent Wetland Evolution in the Hudson River Estuary

SEDIMENTARY PROCESSES INFLUENCING DIVERGENT WETLAND EVOLUTION IN THE HUDSON RIVER ESTUARY

A Thesis Presented

By

Kelly McKeon

Submitted to the Graduate School of the
University of Massachusetts Amherst in
partial fulfillment of the requirements for
the degree of

MASTER OF SCIENCE

September 2021

Geosciences

SEDIMENTARY PROCESSES INFLUENCING DIVERGENT WETLAND EVOLUTION IN THE HUDSON RIVER ESTUARY

A Thesis Presented

By

Kelly McKeon

Approved as to style and content by:

_____
Jonathan Woodruff, Chair

_____
Brian Yellen, Member

_____
Timothy Cook, Member

_____
Stephen Burns, Department Head
Department of Geosciences

ACKNOWLEDGEMENTS

We would like to acknowledge the entire staff at HRNERR over the past twenty years that has collected and made publicly available the dataset used for this study. We thank Brian Arnold, Frances Griswold, Charlotte Wiman, Bob Newton, and Erik Kiviat for their assistance with fieldwork, and Charlotte Wiman and Katherine Castagno for discussion and comments on an early version of the manuscript. This work was supported by a Northeast Climate Adaptation Science Center Graduate Fellowship and a National Science Foundation Graduate Research Fellowship awarded to graduate student Kelly McKeon.

We acknowledge that the land we conducted research on, currently known as New York State, is ancestral land of the Mohican and Mohawk tribes, which was stolen by Europeans during the colonization period beginning in the 1600's. The Hudson River has been used by countless Indigenous peoples, especially those from the Haudenosaunee (Iroquois) and Algonquian Confederacies, as a meeting point and trade highway throughout the Holocene. We would like to acknowledge the stewardship of this land by native peoples, and the impact they had and continue to have on the form and function of the Hudson River Estuary.

ABSTRACT

SEDIMENTARY PROCESSES INFLUENCING DIVERGENT WETLAND EVOLUTION IN THE HUDSON RIVER ESTUARY

September 2021

Kelly McKeon, B.S., Northeastern University

M.S., University of Massachusetts Amherst

Directed by: Dr. Jonathan D. Woodruff

Consistent shoreline development and urbanization have historically resulted in the loss of wetlands. However, some construction activities have inadvertently resulted in the emergence of new tidal wetlands, with prominent examples of such anthropogenic wetlands found within the Hudson River Estuary. Here, we utilize two of these human-induced tidal wetlands to explore the sedimentary and hydrologic conditions driving wetland development from a restoration perspective. Tivoli North Bay is an emergent freshwater tidal marsh, while Tivoli South Bay is an intertidal mudflat with vegetation restricted to the seasonal growth of aquatic vegetation during summer months. Using a combination of sediment traps, cores, and tidal flux measurements, we present highly resolved sediment budgets from two protected bays and parameterize trapping processes responsible for their divergent wetland evolution. Utilizing a 16-year tidal flux dataset, we observe net sediment trapping in Tivoli North for most years, with

consistent trapping throughout the year. Conversely, sediment flux measurements at Tivoli South reveal net sediment loss over the study period, with trapping constrained to the summer months before being surpassed by large sediment exports in the fall and early spring. The timing of the transition from sediment import to export marks the end of the invasive water chestnut growing season and the onset of the associated exodus of both sediment and organic material from Tivoli South. When sediment cores collected for this study are compared to sediment cores collected in 1996, ^{137}Cs profiles confirm little to no sediment accumulation in Tivoli South over the previous two decades. These results support the hypothesis that water chestnut is serving to inhibit sediment trapping and facilitate sediment erosion, preventing marsh development in Tivoli South. The longevity of this dataset highlights the capacity of aquatic vegetation to regulate sediment exchange and geomorphology in enclosed bays when provided an opportunity to colonize. Results of this project provide evidence to inform the management of restoration projects in river systems with freshwater tidal wetlands, especially those affected by invasive species of aquatic vegetation. In bays where tidal sediment supply is not limited, water chestnut removal may present a viable strategy to facilitate marsh restoration.

TABLE OF CONTENTS

CHAPTER 2

LIST OF TABLES

LIST OF FIGURES

CHAPTER 1
EMERGENT AQUATIC VEGETATION MODULATES SEDIMENT TRANSPORT AND TRAPPING IN FRESHWATER TIDAL WETLANDS

1.1 Introduction

In addition to their intrinsic value, the ecosystem functions delivered by wetlands are numerous. Wetlands sequester carbon and pollutants while sheltering communities from coastal flooding, and marsh vegetation acts as a natural filter for improving water quality while providing critical habitat for economically relevant species (Arrigoni et al., 2008; Barbier et al., 2011; Gedan et al., 2011; Knutson et al., 1982; Loomis and Craft, 2010; Minello et al., 2012; Merrill et al., 2002). However, these systems are ephemeral landscape features that exist only under a narrow range of sedimentary and hydrodynamic conditions, leaving them especially vulnerable to environmental changes (Fagherazzi, 2013). Coastal development has led to the destruction of wetlands while increased population concentrated at the coast magnifies the impacts of these losses (Baldwin, 2004; Barendregt et al., 2006; Mitsch and Gosselink, 2000). Because the benefits of tidal marshes to coastal resilience are well understood, marsh restoration efforts that engineer sediment and vegetation to re-establish these natural buffers have become integral to coastal management plans (Baldwin, 2004; Barendregt et al., 2006; Beauchard et al., 2011). Interest in such wetland restoration projects has grown consistently in the face of threats including sea level rise, increased storminess, urbanization, reduced sediment supply, and habitat destruction (Beckett et al., 2016; Howes et al., 2010; Spencer et al., 2016). In response

to these threats, billions of dollars have been invested in creating and restoring marshes around the country (HRECRP 2016, 2018; NFWF, 2014). Many of these proposed efforts remain untested and the current body of knowledge surrounding environmental conditions that reinforce or hinder wetland development remains limited.

The mouth of the Hudson River Estuary lies adjacent to New York City, the largest metropolitan center in the United States, and home to 6% of the US population (US Census Bureau, 2011). The growing population density in proximity to the Hudson River, and to the coast, has rendered the New York metropolitan area increasingly susceptible to coastal hazards that may be mitigated by the ecosystem functions of tidal wetlands. This has made Hudson River Estuary wetland restoration efforts especially pertinent. In the Lower Hudson River alone, collective restoration plans call for $3.5 billion towards the creation of 5,700 acres of new tidal marshes over the next 30 years (HRECRP, 2016,2018). While there is a large body of research covering the influence of sedimentary dynamics on wetland evolution in coastal salt marsh environments, freshwater tidal wetlands are understudied in comparison to their saline counterparts (Tabak et al., 2016; Whigham et al., 2009). Despite the similar ecosystem services delivered by freshwater tidal wetlands, less is known about the mechanisms controlling marsh growth along tidal rivers (Nardin, 2016; Temmerman, 2003). For restoration investments to be effective in the Hudson River Estuary and other analogous systems, a more comprehensive awareness of sediment transport in these systems is necessary.

Recent work in the Hudson has shown that anthropogenic shoreline modifications have incidentally resulted in the emergence of new tidal wetlands (Yellen et al., 2020). While some human land-use changes have been suggested to encourage the expansion of wetlands in saline environments (Kirwan, 2011), the study of this mechanism in freshwater tidal wetlands is more novel. The Hudson River Estuary has been consistently subjected to industrial-scale coastal engineering and environmental manipulation for over 400 years. Construction projects along the Hudson River including damming, railroad construction, shoreline armoring, and the dumping of spoils from dredge channelization have all created new backwater areas that more effectively trap sediment (Bruegel, 2002; Collins and Miller, 2012; Miller et al., 2006; Ralston et al., 2019; Squires, 1992). Intertidal vegetation will only establish and nucleate a marsh when the intertidal surface meets a minimum threshold elevation (Broome et al., 2019). The abrupt changes to the shoreline geomorphology in the Hudson have reduced hydrodynamic energy in off-river waterbodies and allowed for rapid sediment accumulation to reach this threshold elevation quickly (Yellen et al., 2020). These newly sheltered backwater environments with high accumulation rates have provided opportune locations for the prompt initiation of a variety of wetlands at sites where open water previously dominated.

Over 50% of tidal wetlands on the Hudson River have arisen due to this mechanism within the last 150 years, demonstrating the capacity for human interference in shoreline sedimentary processes to quickly yield new wetlands in tidal rivers (Yellen et al., 2020). However, not all backwater environments have transitioned

to marshes, and the mechanisms underlying differential development of wetlands require further investigation. Identifying the conditions that cause some sheltered settings to convert to marsh while others remain mudflat is of great value to the marsh restoration community, who are actively engaged in creating new tidal marshes to replace those that have been lost to development and land reclamation (Ganju et al., 2019; Reed et al., 2018). The Tivoli Bays reside within the freshwater tidal reach of the Hudson, 157-160 km up from the mouth of the estuary (Figure 1). Both bays were cut off from the Hudson mainstem via railroad construction in the 1850s; however, despite similar geomorphologies, hydrodynamic conditions, and sediment supplies, Tivoli North has an extensive emergent marsh while Tivoli South is a mudflat. Here, we present results from these adjacent Tivoli North and South bays with divergent marsh and mudflat morphologies to elucidate the sedimentary, hydrological, and ecological forces driving wetland development trajectories.

Previous research into long-term accumulation rates at the Tivoli Bays utilized both simple hydrodynamic models and sedimentary observations to predict rapid sediment accretion and marsh area expansion under future sea level rise scenarios (Benoit et al., 1999; Tabak et al., 2016; Yellen et al., 2020). While much emphasis has been placed on sedimentation rates in marsh restoration projects, variable marsh establishment at these bays demonstrates that a high sediment supply is not the dominant factor driving marsh evolution, nor is the pace of sea level rise (Baldwin et al., 2019; Ganju et al., 2015). Here, we supplement previous results with additional sediment cores and hydrological data. We deployed sediment traps and returned to

sediment core locations from 1996 to quantify recent deposition and diagnose changes in sediment supply and accumulation rates over the past two decades. Alongside these updated deposition rates, we employed a 16-year dataset of tidal sediment flux at 15-minute resolution to create detailed sediment budgets in both bays. The longevity of this dataset allows us to create extended records of sediment exchange with high temporal resolution, revealing seasonal differences between sedimentary processes in the marsh and the mudflat that appear to be influenced by the life cycle of invasive species *Trapa natans*, which we will refer to as water chestnut throughout this paper.

While submerged aquatic vegetation is broadly known to moderate turbidity in coastal and aquatic settings, little research has investigated the impacts of submerged or emergent aquatic vegetation on water flow and sediment exchange in freshwater tidal settings (Crooks, 2002; Madsen et al., 2001; Work et al., 2021). A modest body of research in California, USA has identified an important link between submerged aquatic vegetation and downstream turbidity in tidal rivers, and we propose a similar mechanism operating in the Hudson River Estuary, where the presence of aquatic vegetation traps sediment and reduces downstream turbidity (Hestir et al., 2016; Schoellhamer et al., 2012; Work et al., 2021). Existing literature on the topic has focused on seagrasses and a few freshwater species, including the invasive *Egeria densa* (Brazilian waterweed), which has demonstrated the capacity to significantly alter the form and function of wetland ecosystems (Ferrari et al., 2014; Hestir et al., 2016; Work et al., 2021). This is the first study to explore the influence of water chestnut on sediment exchange in freshwater tidal wetlands on the east coast of the United States,

highlighting the potential for long-term geomorphological impacts resulting from water chestnut invasion in Northeast tidal rivers.

1.2 Study Site

1.2.1 Hudson River Estuary

At 507km in length, the Hudson River drains a 38,000 km^2 watershed area, and its estuary stretches 243km upriver from Battery Park in New York City, to Troy, NY (Figure 1). Mean tidal range at the mouth of the river is ~1.4 m, decreasing to ~1 m at 90 km upriver before increasing again to 1.6 m at Troy (243 km) (Ralston et al., 2019). The extent of the salinity intrusion varies with discharge, fluctuating between 40 km upriver during high discharge, to as far as 120 km upriver during extreme low discharge (Bowen and Geyer, 2003; Ralston et al., 2008). The Mohawk River and Upper Hudson (above Troy, NY) drain roughly 60% of the estuarine watershed, with a mean discharge of approximately 420 m^3/s (Figure 1). Recent sediment discharge estimates determine approximately 1.2 Mt/yr is delivered to the estuary (Ralston et al., 2021). In New York Harbor, current rates of sea level rise stand around 3mm/yr, with 40-190 cm of total sea level rise expected over the next century (Horton, 2015; Kemp, 2017; Kopp, 2013).

1.2.2 Anthropogenic Modifications to the Estuary

The US Industrial Revolution in the mid-nineteenth century ushered in a series of large-scale river engineering operations to connect the interior of North America to the Atlantic Coast via rail and canal. The main Hudson River channel has been consistently dredged and deepened since the 1800s to accommodate increasingly large vessels

(Collins and Miller, 2012; Miller et al., 2006). Many of the dredge spoils from these navigation projects were dumped on shallow shoals along the margins of the channel, creating new intertidal habitats in the upper reaches of the estuary (Miller et al., 2006, Yellen et al., 2020). Coincident with increased channel deepening, shoreline modifications further affected sediment transport at the river's edges. The Hudson River Railroad was constructed in 1851 on the eastern shoreline of the river, connecting New York City to Troy (Aggarwala, 1993) (Figure 1). This study will focus on two wetlands that have developed in two adjacent embayments separated from the main river by railroad construction. A further discussion of anthropogenic modifications to the estuary and how they have affected sedimentation in off-river waterbodies is available in supplemental material.

1.2.3 Wetlands in the Hudson River Estuary

The Hudson River Estuary is unique in that most of the wetland area is tidally influenced with little to no saline intrusion. Over 80% of the wetlands in the Hudson are freshwater, making the Hudson River Estuary one of the highest concentrations of freshwater tidal wetlands in the eastern United States (Geyer and Chant, 2006; Kiviat et al., 2006). Furthermore, more than half of the wetlands in the estuary have formed over the past two centuries due to anthropogenic estuary modifications including dredging and subsequent dumping, as well as dike and railroad construction (Yellen et al., 2020). Simple models of hydrodynamic exchange show that Hudson River wetlands possess a high capacity for expansion in nearly all sea level rise scenarios (Tabak et al., 2016). Under the current scenario, nearly half of these wetlands are predicted to undergo a

class change (e.g. convert from high marsh to low marsh), but fewer than 15% are expected to drown. Resilient wetlands (expected to expand in area or convert to a different marsh type) are considered the highest priority for conservation and restoration efforts, and more than half of the wetland areas along the Hudson are protected by both public and private agencies (Tabak et al., 2016). Here, we will examine two of these publicly protected wetland locations with rigorous conservation plans.

1.2.4 Tivoli Bays

The focus of this study is the Tivoli Bays (river km 157-160), two adjacent freshwater tidal wetlands on the eastern shore of the Hudson that were simultaneously impounded on their western edges by the construction of the Hudson River Railroad in 1851 (Aggarwala, 1993). The placement of the railroad berm constrained water flow in and out of the bays to five culvert openings underneath the railroad, with two in Tivoli North and three in Tivoli South (Figure 1). This drastically reduced the wave and fluvial energy in both bays, increasing the trapping efficiency of the embayments and facilitating a rapid increase in elevation that converted open water coves to shallow intertidal backwaters within a few decades (Yellen et al., 2020). Tivoli North and Tivoli South are comparable in size (1.45km^2 and 1.05km^2, respectively) and tidal range (1.2 m) and are separated in the north-south direction by a tombolo extending to Cruger Island (Figure 1). Two smaller tributaries drain separately into the eastern side of the two bays (Stony Creek to Tivoli North and Saw Kill to Tivoli South). Stony Creek and Saw Kill have similar watershed areas of approximately 60 km^2 and 69 km^2, respectively.

Since the 1800s, humans have utilized the Saw Kill watershed for agriculture and the water powered processes associated with it, including mills and dams. Today, there is a water treatment plant associated with Bard College on the Saw Kill. While there is preliminary evidence that agricultural operations have not impacted sediment discharge to the bays, the impact of these watershed modifications on sediment yields is still uncertain (Ralston et al., 2021).

Despite comparable geomorphic characteristics, the vegetation compositions at Tivoli North and Tivoli South are markedly different. Tivoli North supports a stable cattail marsh, with 95% of its vegetation comprised of native *Typha angustifolia*. Historical topographic maps indicate that Tivoli North had reached its present marsh extent by the early 1930s (Supplemental Figure 7). In contrast, Tivoli South is 95% open water and intertidal mudflat. In both bays the remaining 5% cover is a mixture of arrowhead (*Sagittaria* sp.), spatterdock (*Nuphar lutea*), and water celery (*Vallisneria americana*) (Sritrairat et al., 2012; Yellen et al., 2020). From late summer to early fall, open water areas of Tivoli South are dominated by the invasive water chestnut species *Trapa natans*. Previous studies have identified a higher organic content and lower grain size in Tivoli North when compared to Tivoli South. These studies estimated accumulation rates between 0.7 and 1.0 cm/yr in Tivoli North, and rates between 0.5 and 2.9 cm/yr in TVS (Benoit et al., 1999; Sritrairat et al., 2012; Yellen et al., 2020) (Supplemental Figures 1 and 2).

1.2.5 Invasion of Water Chestnut

Water chestnut is a fast-growing aquatic annual plant native to Europe, Africa, and Asia, which grows best in shallow, nutrient-rich waters. Water chestnut was first introduced to the United States in 1859, near Concord, MA, and can now be found throughout the Northeast US in tidal river systems including the Hudson, Connecticut, and Chesapeake (Hummel and Kiviat, 2004; Naylor, 2003). The first documentation of significant invasion in the Hudson was in the late 1930s, and by 1950 water chestnut was pervasive, found in dense monospecific stands in bays including Tivoli South (Hummel and Kiviat, 2004; Strayer, 2010). The water chestnut plant is characterized by subsurface stems that may extend up to 5m to the water surface where they bear floating leaves (Figure 2B). The stems are secured in the substrate by lower roots and the hull of the seed pod from which it germinated. Chestnut plants produce between 10 to 15 heavy nuts each, which they drop between the months of mid-July and September. The nuts have a hard, sharp exterior, and can lay dormant in the sediment for up to 12 years, before they germinate at a temperature of 12°C (Hummel and Kiviat, 2004; Naylor, 2003). Water chestnut seeds generally begin to sprout in early June, prompting full, dense coverage of Tivoli South between July and September, with the biomass peak in August (Findlay et al., 1990; personal observation). In late September complete die-off of the chestnut stand occurs, and large wracks of dead water chestnut are rapidly exported out the culverts, returning the bay to open water within a matter of weeks (Findlay et al., 1990, Figure 2).

1.3 Methods

1.3.1 Water Column Observations

This study utilized a public dataset from the Hudson River National Estuarine Research Reserve (HRNERR) to assess sediment fluxes at the Tivoli Bays. Data was accessed from the Hudson River Environmental Conditions Observing System Centralized Data Management Office (CDMO). All HRNERR data and metadata are available at cdmo.baruch.sc.edu. Five total cuts underneath the Hudson River Railroad connect the Tivoli Bays to the main Hudson River. There are three culverts in Tivoli South and two culverts in Tivoli North, with all culverts measuring ~25 m across. HRNERR long-term monitoring stations are located at the northern culvert in Tivoli South (42° 1' 37.34 N, 73° 55' 33.45 W), the southern culvert in Tivoli North (42° 2' 11.56 N, 73° 55' 31.17 W), at the Stony Creek Tributary (42° 2' 46.68 N, 73° 54' 38.88 W), and at the Saw Kill Tributary (42° 2' 46.68 N, 73° 54' 38.88 W) (Figure 1).

These stations collect a depth and turbidity measurement every 15 minutes from the months of April – December, and we use data from 2004-2019 for this study. Water samples were also collected by HRNERR at Tivoli South, Stony Creek, and Saw Kill, and filtered, dried, and weighed to measure suspended sediment concentrations (SSC). SSC was measured over two tidal cycles per month at Tivoli South from 2016-2019, and two replicates per month were collected at Stony Creek and Saw Kill from 2016-2019. All HRNERR measurements were evaluated for quality control by the CDMO, and all measurements with quality control flags due to instrument fouling, malfunction, or data anomalies, were removed from the analysis. A description of how excluded values were

handled is available in Supplemental Methods 2.2.1. We deployed water level loggers and current-tiltmeters at four of the five culverts from July – October 2020, with mid-deployment data downloaded once in August (Figure 1). This secondary instrumentation confirmed a standing tide system where slack water occurred at high and low tide, and in which water fluxes were comparable between culverts within Tivoli North and Tivoli South. Therefore, high-resolution HRNERR water level and turbidity measurements from the single measured culvert in Tivoli North and Tivoli South were assumed representative of all culverts in each respective bay. Further explanation of this justification is available in Supplemental Methods.

1.3.2 Turbidity-SSC Calibration

Linear regressions were used to calibrate turbidity to SSC, in which we regressed in-situ turbidity to in-situ SSC. SSC was measured by HRNERR within 15 minutes of a turbidity measurement, and turbidity values were interpolated from the continuous 15-minute measurements to match the exact time of SSC collection. At Tivoli South, the SSC (mg/L) was equivalent to $1.2x + 7$ where x is turbidity (NTU) ($r^2 = 0.52$, n = 329) (Figure 3). Measurements at Stony Creek and Saw Kill were combined into one regression to improve the fit, where SSC (mg/L) was found equivalent to 1.2 times the turbidity (NTU) ($r^2 = 0.66$, n = 113) (Figure 3). Loss-on-ignition was employed to evaluate the relative fraction of clastic sediments and organics represented by turbidity values. All filters used in the SSC calibration were weighed dry, combusted at 550°C for four hours, and re-weighed to obtain clastic sediment mass. Organics did not significantly skew turbidity

values, and all turbidity values passing the quality control check were included as-is in the analysis. More details on this determination are available in Supplemental Methods.

1.3.3 Flux calculations

To estimate tidal flux in each bay (Q_{tide}, m^3/s), we utilized a similar model to that in Boon (1975), which relates discharge through a marsh channel to change in tidal elevation. Here, we combine the time-series of HRNERR depth measurements with USGS lidar (NAVD88, 1 m^2 resolution, NOAA 2014) elevations in each bay to calculate tidally varying flow through Tivoli North and South culverts. Lidar elevation data was cross-checked against Real Time Kinematic (RTK) point elevation measurements, and it was determined that lidar overestimated elevation in both the marsh and the mudflat, by 0.3 m and 0.1 m, respectively (Supplemental Figure 4). The tidal prism was calculated from corrected lidar elevations and total tidally varying flow through the respective culverts at Tivoli North and Tivoli South was determined by the equation $Q_{tide} = \frac{dh}{dt} A$, where *A* is the tidally varying area of tidal flat in Tivoli South and marsh in Tivoli North flooded at each tidal stage, *h* is water depth, and *t* is time (Supplemental Figure 5). We conducted Acoustic Doppler Current Profiler (ADCP) water flux surveys at all culverts in October 2020, which validated the equivalency of our depth-derived discharge approximations across culverts (Supplemental Figure 6).

To calculate fluvial discharge from side tributaries, we fit water depth at Stony Creek to freshwater discharge from the nearby USGS gauge at Roeliff Jansen (Gage 01362182, 42°09’08” N, 73°50’38” W, Figure 1) for the years 2011-2013. We obtain an

exponential relationship between depth in meters at Stony Creek (h_{SC}) from 2004-2019 and discharge at Roeliff Jansen (Q_{r_RJ}, m^3/s) of $Q_{r\_RJ} = 2745\ h_{SC}{}^4$ ($r^2 = 0.60$, n = 753) and scaled by a factor of 0.11 to account for differences in watershed area between Stony Creek and Roeliff Jansen, i.e. $Q_{r\_SC} = 0.11(2745\ h_{SC}{}^4)$ (Figure 3). Mean annual runoff calculated for Stony Creek using this method was consistent with mean annual discharge reported for the region (50 cm/yr, USGS 2016). Because of their similar watershed areas, and an absence of depth measurements at Saw Kill prior to 2011, we assumed river discharge at Stony Creek and Saw Kill to be equivalent while deriving separate SSC time-series based on individual turbidity measurements obtained near the mouth of each respective tributary. Sediment fluxes (Q_s) at the culverts and tributaries were calculated at 15-minute intervals using the SSC, Q_{tide}, and Q_r values approximated above, and then assessed and cumulatively summed on tidal, monthly, and annual timescales.

1.3.4 Sediment Cores

As of 2020, sediment cores had previously been collected in both Tivoli North and Tivoli South by Yellen et al. (2020) and Benoit et al. (1999) (Supplemental Figure 1). To supplement these cores and compare accumulation rates over the past two decades, new cores were collected in August 2020 at eight locations in Tivoli South, as close to the Benoit 1999 core locations as was feasible. All cores were collected at low tide using a 6.3 cm diameter gouge corer to minimize compaction. For most locations, we

successfully collected three overlapping 1 m drives. For locations where we could not retrieve three full drives, we drove until refusal.

Relative age controls were established for two cores (M7 and M8) using downcore profiles of ^{137}Cs obtained via gamma spectroscopy. Cores M7 and M8 were selected for their proximity to cores B7 and B8 originally collected by Benoit et al. (1999) in 1996, and for the quality and reproducibility of their ^{137}Cs profiles (see Figure 1 for locations). The upper meter of each core was sampled every 10 cm for ~2 cm^3 of sediment. Samples were dried, crushed, and counted for at least 48 hours on a Canberra GL2020R Low Energy Germanium Detector. We make use of the 1954 ^{137}Cs onset and the 1963 ^{137}Cs peak as our primary stratigraphic markers and compare the depth of these markers at the time of collection in 2020 to that observed originally in cores collected in 1996 by Benoit et al. (1999) to derive the amount of deposition or erosion over the past 24 years.

1.3.5 Sediment Traps

Sediment traps were installed in two transects across the marsh platform in Tivoli North, with five stations in each transect (Figure 1). At each station, five 50mL centrifuge tubes with 2.7 cm diameters were pushed into the sediment until level with the marsh platform. Traps at Transect 1 were deployed from June-October, while traps at Transect 2 were deployed from August-October. Sediments collected in the traps underwent loss-on-ignition following the same method described above for water column filters. Clastic sediment mass was divided by the surface area of the trap and the

length of time deployed to calculate the deposition rate over each trap's deployment period, and we report the average of those rates here (Table 1). Further discussion of sediment trap data collection and processing is available in Supplemental Methods.

1.4 Results

1.4.1 Sediment Fluxes

We compared 16 years of turbidity measurements at the open water Tivoli South site to the vegetated Tivoli North site at the 15-minute resolution of our measurements, as well as tidally, monthly, and annually. At high-resolution timescales, turbidity values at the culverts were generally comparable— between the time-series of their individual 15-minute measurements, mean values of flood tide turbidities, and median values of annual turbidities. However, when we evaluated the 16-year median of daily average turbidity, turbidity differed between bays on a seasonal basis, with Tivoli North having consistently higher turbidity from the months of June to mid-October by as much as 10 NTU (Figure 4). Median turbidity values for the entire dataset are 12NTU in Tivoli North and 9 NTU in Tivoli South. Between flood and ebb tide, we observed a higher turbidity on flood tide in Tivoli North in the winter and fall, while flood and ebb turbidities remained roughly equivalent during the summer. In contrast, Tivoli South exhibited a seasonal divergence in flood and ebb turbidities, in which ebb turbidity is higher than flood in spring and fall, while ebb turbidity is depressed from mid-July to mid-October (Figure 4).

On tidal timescales, we found that SSC is tidally controlled in Tivoli North, with median SSC peaking during flood tide at ~ 25 mg/L, before decreasing on the ebb tide. In contrast, median SSC in Tivoli South remains between ~ 15 mg/L and ~ 20 mg/L throughout the duration of the tidal cycle, with a slight peak during the ebb tide. When we integrate these SSC measurements with water flux at the culverts, we observe flood tide dominated sediment flux at Tivoli North and ebb tide dominated sediment flux at Tivoli South, where the tidal cycle mean of all flux measurements equals 43.1 kg at Tivoli North and -43.2 kg at Tivoli South (Figure 5).

Across all timescales at the tributaries, we observe higher turbidity in Stony Creek, with greater variability and elevated extremes (Figure 4). From 2004-2019, we estimate ~ 9000 tons of sediment were delivered to Tivoli North from Stony Creek, and ~ 4000 tons of sediment were delivered to Tivoli South from Saw Kill. These calculations place annual sediment yields for Stony Creek and Saw Kill at ~ 10 tons/km^2/yr, and ~ 4 tons/km^2/yr, respectively.

1.4.2 Net Budgets

We cumulatively summed the 15-minute Q_s values from the culverts and tributaries to obtain annual values of net sediment import at both the marsh at Tivoli North and the mudflat at Tivoli South. Annual sediment delivery from Stony Creek to Tivoli North ranged between 100 and 1500 tons. At Saw Kill, annual sediment supply ranged between 40 and 600 tons. For sediment transport at the culverts, the tidal component produced both positive and negative annual fluxes in Tivoli North and Tivoli

South. We added the sediment inputs from the tributaries to the sediment flux at the culverts to obtain a net sediment flux for each bay. In years where total net sediment flux is negative, we assume sediment export, and in years where net sediment flux is positive, we assume sediment import (Figure 6).

Of the 16 years included in this study, Tivoli North showed net sediment import for all but two years (2014 and 2019), with 2015 and 2016 at equilibrium (no import or export). In contrast, Tivoli South exhibited net sediment export for eight years (2007,2012,2014-2017, and 2019), import for 3 (2005-2006, and 2010), and equilibrium for six (2004, 2008-2009, 2011, 2013, and 2018). There is a noticeable shift in the budgets of both bays in 2014, where it appears that both Tivoli North and South consistently export after the year 2014 (Figure 6). We attribute this change in net annual flux to the decrease in turbidity ratio in the Hudson River noted by Ralston et al. (2020) over the years 2014-2018. Cumulative sediment flux over the entire dataset shows that over 21,000 tons of sediment was added to Tivoli North between 2004 and 2020, while Tivoli South lost over 3000 tons of sediment over the same interval (Figure 6). Using theestimate of net sediment import to Tivoli North in combination with total wetland area, we calculated a mineral accumulation rate of 0.10 $g/cm^2/yr$ at Tivoli North. Comparatively, the eight sediment trap locations in two marsh transects generated a mean annual accretion rate of 0.18 $g/cm^2/yr$ in Tivoli North. However, when the station closest to the channel in Transect 2 is removed from the site average, our sediment trap data closely aligns with our water column data, placing mean annual accretion at 0.13 $g/cm^2/yr$ (Figure 1, Table 1).

1.4.3 Erosion Rate at Tivoli South

We make use of ^{137}Cs as a chronological marker in two sediment cores, M7 and M8, to quantify sediment accumulation in Tivoli South since 1996 (see Figure 1 for locations). The core further from the channel, M7, displayed an onset of ^{137}Cs between 24 and 30cm, with a peak between 17 and 21cm (Figure 7). We interpret this onset of ^{137}Cs to the year 1954 CE, and the ~ 20cm peak to represent the year 1963 CE (Appleby, 2001). In core M8, located directly next to the tidal channel, we observe this 1954 CE onset of ^{137}Cs between 13 and 15cm, and the 1963 CE peak at 10cm. When plotted next to ^{137}Cs downcore data from Benoit et al. (1999, cores B7 and B8), these stratigraphic markers are shallower in the 2020 cores than they were in 1996, the year of collection in Benoit et al. 1999 (Figure 7). The offset between ^{137}Cs peaks in M8 and B8 suggests roughly 12 cm of sediment erosion at this location between 1996 and 2020, with no new sediment accumulation at the M7 location since 1996.

1.4.4 Seasonality of Sediment Delivery

Seasonal trends in turbidity at Tivoli North and Tivoli South became apparent when we examined the median of the 16 years of daily turbidity values, for each day of the annual sampling period (April-December, Figure 4). Tivoli North and Tivoli South had nearly the same turbidity values from April-June. In June, the culverts diverged in median turbidity, with Tivoli South consistently remaining ~ 5 NTU lower than Tivoli North until late October. In November, this pattern shifted so that turbidity was higher

at Tivoli South, with a notable peak at the end of October that was not present in Tivoli North (Figure 4).

When Q_s was cumulatively summed by month, a strong seasonal trend appeared in the Tivoli South mudflat that was not present in the marsh at Tivoli North. This trend in Tivoli South is characterized by net sediment export in April and May, followed by net import from June-September, with a transition month in October before returning to net export in November and December. The seasonality of net sediment flux in Tivoli South closely tracks the life cycle of water chestnut in the bay, which emerges in June, begins to die in October, and is entirely absent from the bay by November (Figure 8). In Tivoli North however, we observed positive median monthly sediment accumulations for all months except for April, with peak import in November.

Seasonality in tributary sediment delivery likewise differed between the marsh at Tivoli North and the mudflat at Tivoli South. Median monthly sums of Q_s in Saw Kill were low, but consistent throughout the year, with only minor variability in the range of cumulative sediment delivery to Tivoli South (Figure 8). In Stony Creek, there was a bimodal seasonality to monthly sediment discharge, with peaks in both May and October and a larger spread of monthly sediment delivery values to Tivoli North. This seasonality of sediment discharge at Stony Creek aligns with seasonal sediment trapping in Tivoli North, with peaks in both spring and fall (Figure 8).

1.5 Discussion

1.5.1 Spatial and Temporal Variability in Accumulation Rates

The sediment budgets of this study represent semi-quantitative assessments of accumulation or erosion over the past two decades at Tivoli North and Tivoli South. Flux measurements presented here are not intended to be taken as fixed values. Rather, the focus of this analysis is centered on comparing differences between the two sites based on a common suite of measurements with high spatial and temporal coverage. We urge caution in treating these values as absolute measurements of accumulation or erosion. Using multiple lines of evidence, we find semi-quantitative measurements of sediment flux inferred from water column monitoring, sediment cores, and sediment traps all converge on the same net trends in sediment accumulation in the Tivoli Bays.

When we compare our SSC-derived estimates of sediment delivery and trapping in the Tivoli Bays to previous estimates calculated from sediment core age models, we find our assessment of sediment flux signifies lower accumulation rates than formerly assumed at these locations (Benoit et al., 1999; Sritrairat et al., 2012; Yellen et al., 2020). The previously inferred annual minerogenic accretion rate since 1954 of 0.2 $g/cm^2/yr$ at Tivoli North translated to over 1 cm per year in vertical accretion on the marsh (Yellen et al., 2020). While exclusion of data between December and April in our dataset may mean our estimate is on the low end, those sediment core-based accumulation rates are more than double the 0.1 $g/cm^2/yr$ average we infer from sediment trap measurements in Tivoli North. It is possible that springtime sediment flux

could contribute additional inputs to this sediment budget, although unlikely that it would be enough to reconcile this 0.1 g/cm^2/yr discrepancy. Furthermore, we would expect minimal accumulation during the winter months and potentially even erosion due to ice rafting during the early spring (Neubauer et al., 2002; Pasternack and Brush, 2001; Ralston and Geyer, 2009; Wall et al., 2008). Thus, we infer our lower rates of mineral accumulation to reflect a decrease in accretion rates between 1850 CE and present day, likely due to the site's transition from an over-deepened embayment directly following railroad construction to its present morphology as a freshwater tidal wetland whose current elevation resides near mean high water with the rate of increase now set by local SLR.

Our calculated export of sediment at Tivoli South is similarly incongruous with previously published sediment core-based accumulation rates. Previous age-depth models published from Tivoli South have estimated accumulation rates between 0.5 cm/yr and 2.9 cm/yr (Benoit et al., 1999; Sritrairat et al., 2012; Yellen et al., 2020) (Supplemental Figure 1). Yet, none of these studies predicted the sediment export we observed from Tivoli South over the past 16 years. Furthermore, the spatial variability in the ^{137}Cs offset between 2020 sediment cores and 1996 sediment cores suggests that locations closer to the channels are now eroding faster than more distal locations (Figure 1, Figure 7). This contrasts with our sediment trap data in the marsh environment, where locations closer to the channel accumulate faster, with accumulation rates decreasing linearly with distance from the channel (Figure 1, Table 1). This paradigm of varied accretion or erosion dictated by channel proximity is widely

observed in marshes with tidal creeks and ditching (Neubauer et al., 2002; Temmerman et al., 2003).

The synthesis of water column, sediment trap, and sediment core data shows that accumulation rates in Tivoli were higher between 1850 and the early 2000's but have now slowed drastically as accommodation space in both bays decreased, even recently flipping to an erosion regime in the mudflat. This is reflected in the gradual decrease in annual sediment accumulation in both bays over the course of our study period (Figure 6). Our estimations of annual sediment budgets also indicate that years of net import and net export exist for both bays, and factors such as river discharge and extreme events have independent and isolated effects on sediment import in each bay, as noted in other studies pertaining to sediment storage in the Hudson River Estuary (Ralston and Geyer, 2009; Wall et al., 2008). This high temporal variability in sediment delivery and storage in small, enclosed bays is easily averaged out of accumulation rates determined by long-term sediment core data, and researchers should exercise caution when using these metrics to inform short-term restoration practices in such dynamic systems.

1.5.2 Role of Water Chestnut in Modulating Mudflat Sediment Transport

High vegetation density is known to increase trapping efficiency and stabilize sediment in freshwater marsh habitats, allowing them to build elevation more effectively (Butzeck et al., 2015; Temmerman et al., 2003). However, the role of seasonal submerged aquatic vegetation in sediment trapping is less studied, and

literature pertaining to the trapping efficiency of water chestnut is scarce. There is preliminary evidence that water chestnut in the Hudson River is effectively trapping sediment on small spatial and tidal scales (Hummel and Findlay, 2006). The seasonal pattern we observe in Tivoli South, where overall turbidity decreases from June-September below that observed at Tivoli North (Figure 4), when water chestnut is present, serves as further evidence that water chestnut is trapping sediment at larger spatial and temporal scales (Figure 4). Here we offer a conceptual approach to sediment transport in a freshwater mudflat environment where water chestnut operates as a seasonal interceptor of sediment, preventing meaningful accumulation and enabling wetland erosion.

When we compare monthly sediment exchange rates in Tivoli North and Tivoli South, the directionality of net sediment flux can be explained by the presence or absence of water-chestnut in the mudflat, which has no effect on trapping in the marsh (Figure 8). While there is little literature describing the seasonality of water chestnut biomass, it is recognized through anecdotal evidence and personal observation that water chestnut begins to appear in June and persists thickly in Tivoli South until early October. Findlay et al. (1990) identified export as the primary fate of water chestnut organic material, and this rapid departure of vegetation after its seasonal death may explain the seasonality of sediment export in Tivoli South. During the month of October, all the water chestnut is quickly exported out the culverts in a matter of weeks, carrying with it much of the sediment it had intercepted over the summer. It is likely that the filamentous lower floating leaves (Figure 2B) are efficient traps of sediment, and this

phenomenon is reflected in both the depressed ebb tide turbidity throughout the summer in Tivoli South, and the anomalous rise in mean turbidity at the end of October in Tivoli South that is not present in Tivoli North (Figure 4). This pattern of seasonal sediment trapping has been described in other freshwater tidal wetlands with floating leaf habitats in the Chesapeake Bay, and there is limited evidence that vegetation may control sediment deposition rates in mudflat locations where river sediment is not limited, which is the case in Tivoli South (Darke and Megonigal, 2003; Pasternack and Brush, 2001).

We propose that the annual life cycle of water chestnut is the primary reason for the opposing geomorphologies of the Tivoli Bays. While water chestnut is present, the finest fraction of sediment settles on its leaves, and the plant becomes visibly covered in clay. When the plant dies, it disturbs the substrate as its roots break free, and large floating wracks of water chestnut transport the sediment affixed to its leaves and trapped in the wrack out to the main Hudson River. Very little debris undergoes decomposition or burial within the bay, limiting the accumulation of organic material in the mudflat substrate (Findlay et al., 1990). Other studies have highlighted the important role of organic material in marsh accretion in freshwater tidal wetlands, with one such study estimating that organic material is responsible for 62% of accretion in a freshwater marsh (Neubauer, 2008). Furthermore, these studies have suggested that an absence of plant litter on the substrate of a mudflat might encourage erosion in winter and spring months due to ice rafting, and during periods of high hydrodynamic activity such as spring tides or elevated flow from side tributaries (Neubauer, 2008; Odum,

1988). The absence of vegetation coverage during winter in Tivoli South may be responsible for the higher sediment exports in the spring than the fall (Figure 8), as unvegetated mudflats have been shown to have high springtime erodibility due to a lack of biological stability that is compounded by a complex variety of secondary hydrologic and ecological factors (Anderson and Black, 1981; Anderson, 2001). Additionally, our estimate of sediment outflux in the fall does not account for sediment trapped in the water chestnut racks, much of which we would expect to be the fine-grained clays and silts. Previous analysis of grain size and organic content in Tivoli North and Tivoli South show that the mudflat has both a higher median grain size and a lower organic content than the marsh, supporting this hypothesis (Yellen et al., 2020) (Supplemental Figure 2). The seasonal death and subsequent rapid export of water chestnut drives the simultaneous loss of both mineral and organic material that creates a dearth of fine-grained organic substrate, preventing further elevation building and limiting the capacity for marsh initiation at this site.

1.5.3 Role of Tributary Sediments in Marsh Development

Freshwater tidal wetlands are known to be higher in terrestrial sourced sediment than salt marshes (Marcus and Kearney, 1991; Odum, 1988). Despite research showing that inundation time during the tidal cycle is the primary driver of sedimentation rates in freshwater tidal wetlands (Butzeck et al., 2015; Neubauer et al., 2002; Odum, 1988; Temmerman et al., 2003), our results suggest that terrestrial sediment inputs may be important enough to adjust wetland morphology in locations that already receive a

robust sediment supply from the main tidal river. The differences in sediment loading from Stony Creek and Saw Kill are puzzling, as the two watersheds appear very similar. A previously published estimate for the entire Tivoli watershed was developed through scaling regional sediment yields by watershed area and estimated annual yield for Tivoli at 100 tons/km^2/yr, distinctly higher than our estimates (Ralston et al., 2021). It is possible that the presence of dams and usage of the Saw Kill for milling and agricultural purposes may have limited the discharge of sediment in this river. Furthermore, the long-term presence of a water treatment plant along the river may have increased nutrients in the bay, making the bay more susceptible to quickly colonizing invasive species (Hummel and Kiviat, 2004; Naylor, 2003). Additionally, the Stony Creek watershed is only 48% forested compared to the Saw Kill's 69% forest cover (USGS, 2016). This higher rate of deforestation may also have a role in Stony Creek's higher sediment yields. By the time water chestnut invasion reached the area in 1930, Tivoli North had already nucleated a marsh (Supplemental Figure 7). The higher sediment load deposited in Tivoli North from Stony Creek may have allowed the northern bay to accumulate more sediment, gaining elevation more rapidly than Tivoli South. While the bays' former geomorphologies appear similar, historical maps from 1863 depict Tivoli South as open water up to 3m deep, while Tivoli North is drawn as land. This cartographical difference suggests a slightly deeper initial bay depth at Tivoli South, which could have amplified the effects of these differing sediment loads on elevation changes in the bays and allowed Tivoli North to reach the critical elevation for marsh establishment before Tivoli South (Supplemental Figure 7). This would have provided an

exclusive opportunity for water chestnut to colonize in Tivoli South, where it currently modulates annual sediment accumulation in the mudflat, preventing a marsh from developing.

1.5.4 Restoration Implications

Previous assessments of wetland resilience in Tivoli Bays utilized both simple model simulations and sediment core data to estimate the fate of both marsh and mudflat under future environmental changes (Tabak et al., 2016; Yellen et al., 2020). It was formerly believed that Tivoli South was accreting sufficient sediment to transition to a marsh in the future, as Tivoli Northhad done a century ago. Our findings suggest the opposite, that both the marsh and the mudflat systems have achieved steady-state morphologies and the mudflat is unlikely to transition to a marsh without significant human intervention. While many freshwater tidal wetlands seem to be accumulating at rates comparable to SLR, Tivoli South is an exception to this trend, as it has not only not kept pace with SLR over the past two decades, but it also appears to be actively eroding. Moreover, we suspect that our calculated rate of export in Tivoli South represents a minimum estimate, as much of the sediment trapped within the water chestnut wrack is not captured in water column turbidity measurements and our analysis does not account for sediment exports via ice rafting. These potential modes of sediment removal represent important research topics for future study.

The results of this study have illuminated the significant impact that water chestnut has on sediment exchange and trapping in enclosed bays and highlighted the

potential large-scale morphological impacts of invasive emergent aquatic vegetation colonization. The presence of water chestnut acts as a seasonal interceptor of sediment, prevents marsh initiation and growth, and facilitates erosion in unvegetated tidal wetlands. The invasion of water chestnut has affected watersheds throughout the Northeast US. However, remediation projects in the Chesapeake Bay have shown that continued manual removal of water chestnut caused over a 99% decline in biomass within four years, leading to a near complete water chestnut eradication (Hummel and Kiviat, 2004; Naylor, 2003).

We hypothesize that tidal marshes were able to establish themselves more quickly in Tivoli North than Tivoli South due to increased sediment input from Stony Creek relative to Saw Kill. This suggests that in certain tidal wetland settings, sediment inputs from terrestrial sources and side-tributaries may have a larger influence over initial marsh development than sediment exchange with the estuary. If it is true that mill dams on the Saw Kill are responsible for its comparatively low sediment yield, it is possible that water chestnut removal in Tivoli South combined with dam removal on the Saw Kill could activate marsh nucleation in Tivoli South. Further exploration of the sedimentary dynamics in this system will be necessary to determine if this is a viable conservation strategy in the Tivoli Bays.

As more focus is placed on the restoration and conservation of tidal wetlands, it is imperative that stakeholders possess an intimate knowledge of the primary geological and ecological factors driving wetland evolution. Literature pertaining to the biology and

ecology of water chestnut as an invasive species is scarce, and research investigating the intersection of this species and sedimentary dynamics is limited. More research is needed into the role of water chestnut in wetland sediment exchange, not just in the Hudson River but in all areas affected by water chestnut invasion. As communities, governments, and private organizations choose where to invest in wetland restoration, creating detailed sediment budgets that incorporate sediment cores and traps, water column measurements, and hydrodynamic modeling that accounts for seasonal vegetation changes, will provide necessary perspective on the potential success of various restoration methods. By incorporating these results into restoration planning, funding for projects may be allocated more strategically to optimize success in future restoration efforts.

1.6 Conclusion

We employed a 16-year tidal flux dataset to quantify sediment transport and trapping at high temporal resolution in two adjacent freshwater tidal wetlands with contrasting geomorphologies. We analyzed fluxes at monthly, annual, and decadal timescales to reveal that the marsh habitat in Tivoli North has trapped over 20,000 tons of sediment over the past two decades, while the mudflat at Tivoli South has exported nearly 3,000 tons of sediment over the same period. Sediment cores and traps from Tivoli North and Tivoli South support this evidence, showing a positive annual accumulation rate in the marsh, while modern sediment cores in Tivoli South show either no accumulation or net sediment erosion when compared to cores from 1996. Cumulatively summed monthly sediment budgets over the study period show constant

trapping in Tivoli North throughout the year. This is contrasted by a seasonal cycle of sediment flux in Tivoli South that is characterized by net sediment import over the summer and net sediment export in the spring and fall. We conclude that the export observed during fall is due to the death and ensuing outflux of water chestnut vegetation and sediment trapped within its biomass, while the absence of vegetation on the mudflat surface during the spring encourages erosion during this period. These results showcase the potential for significant geomorphological impacts in wetlands affected by long-standing invasions of emergent aquatic vegetation and highlight the need for more research into water chestnut sediment trapping when making restoration plans for wetlands in the Hudson River Estuary and other tidal river systems.

1.7. Figures and Tables

1.7.1 Table 1

Transect	Trap	Deposition Rate (g/cm^2/yr)
T1	2	0.064
T1	3	0.189
T1	4	0.206
T2	1	0.500
T2	2	0.096
T2	3	0.061
T2	4	0.057
T2	5	0.234

Table 1. Deposition rates (g/cm^2/yr) calculated from sediment traps in Transect 1 (T1) and Transect 2 (T2). See Figure 1 for locations.

1.7.2 Figure 1

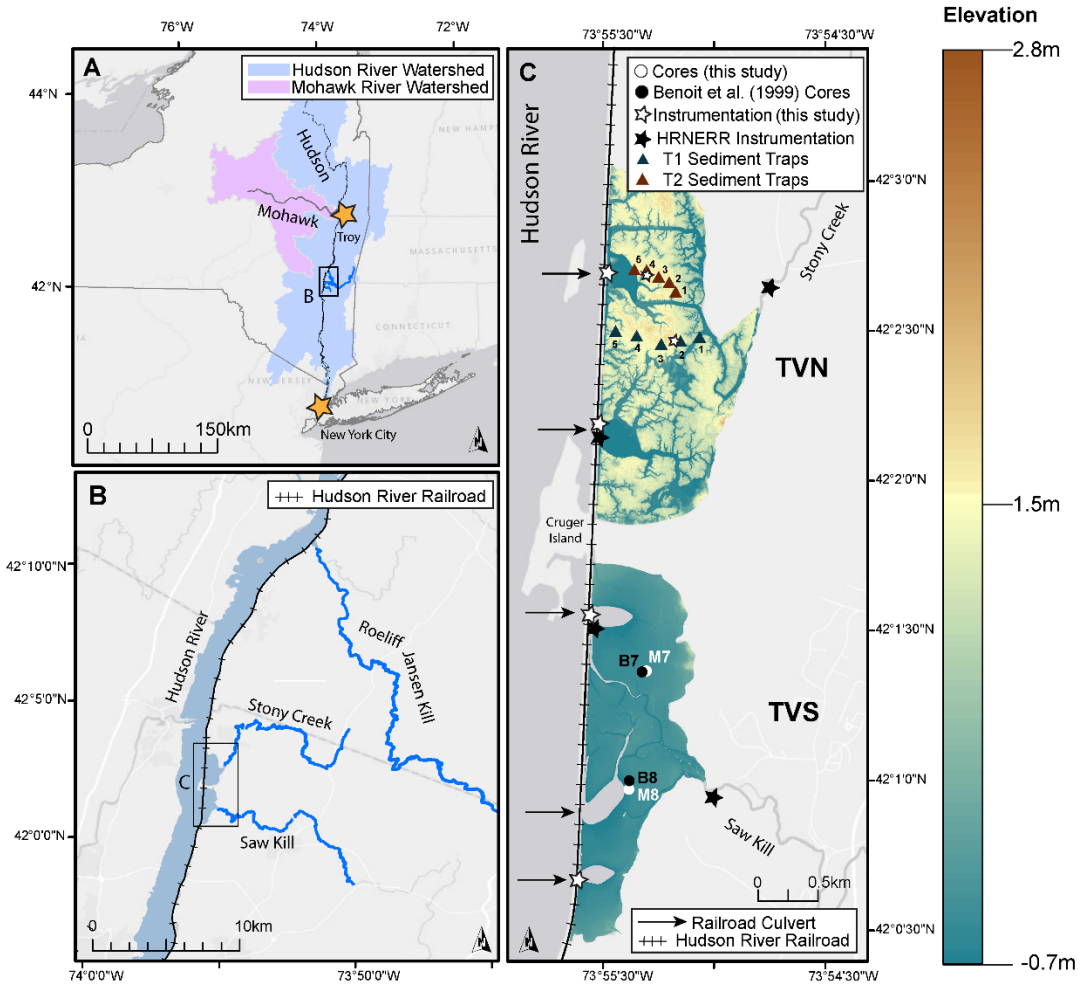

Figure 1. (A) Map of New York State with Hudson River watershed shown in blue. The Mohawk River watershed provides the largest upstream source of sediment to the Hudson River Estuary and is shaded in pink. **(B)** Map of primary tributaries draining into Tivoli North (TVN, Stony Creek) and Tivoli South (TVS, Saw Kill), and Roeliff Jansen Kill where available river discharge was used for stage-discharge calibrations at Stony Creek and Saw Kill. **(C)** Lidar elevations in the Tivoli Bays (NOAA 2014) with sampling locations marked. Black stars depict sites of HRNERR long-term monitoring stations. White stars show locations of turbidity sensors, water level loggers, and current meters deployed from June-October 2020. Cores collected for relative age comparison to Benoit et al. 1999 (black circles) are marked by white circles, and triangles denote sediment traps installed for this study. Black arrows mark pathways for water and sediment exchange underneath the railroad.

1.7.3 Figure 2

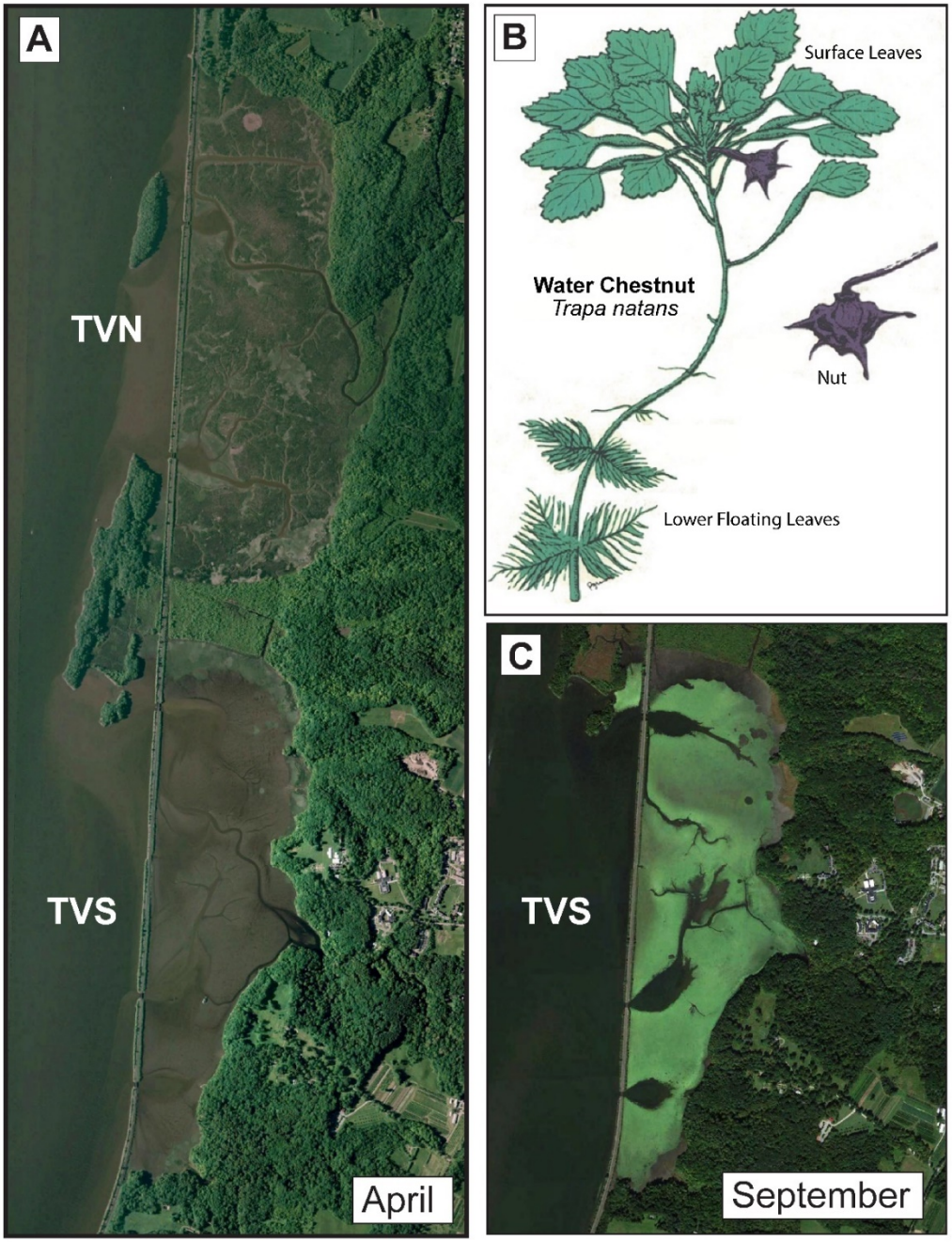

Figure 2. (A) Tivoli Bays in April 2010 (Google Earth), with Tivoli South (TVS) devoid of water chestnut. **(B)** Structure of the water chestnut plant *Trapa natans* (modified from NYSIS, 2019). **(C)** Tivoli South in September 2013, during the height of water chestnut season, visible in bright green.

1.7.4 Figure 3

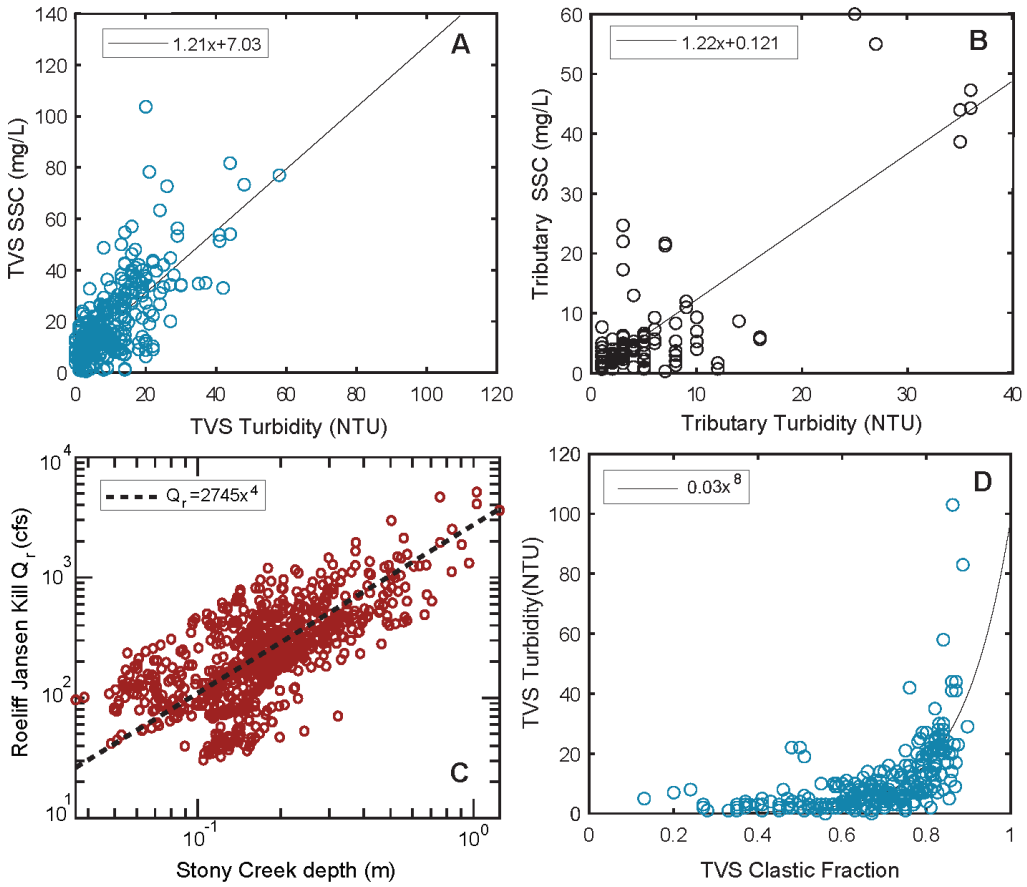

Figure 3. (A) Turbidity vs Total SSC from 2016-2019 at Tivoli South (TVS) culvert, with linear regression shown in black. **(B)** Combined turbidity vs combined SSC at Saw Kill and Stony Creek, with linear regression shown in black. **(C)** Depth at Stony Creek vs discharge (Q_r) at Roeliff Jansen Kill, with power-law fit shown in dotted black. **(D)** Clastic fraction of SSC at Tivoli South vs Tivoli South Turbidity, with power-law fit shown in black.

1.7.5 Figure 4

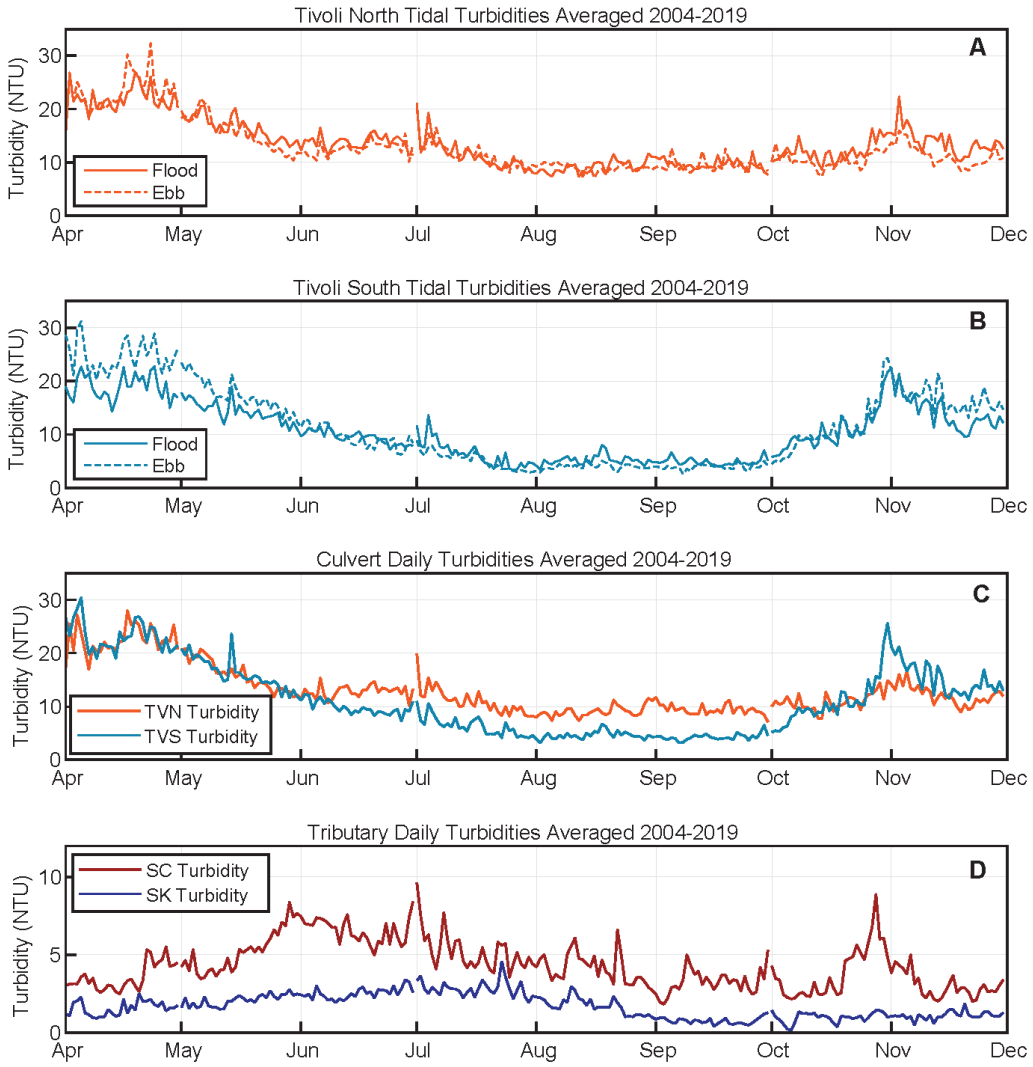

Figure 4. Top two panels show the 16-year median of average flood tide turbidity (NTU) in solid lines and ebb tide turbidity in dashed lines at Tivoli North **(A)** and Tivoli South **(B)**, for each day from April 1 to November 31**.** Bottom two panels show the 16-year median of daily average overall turbidity at Tivoli North (TVN, orange line) and Tivoli South (TVS, blue line) culverts **(C)** and at tributaries Stony Creek (SC, red line) and Saw Kill (blue line) **(D)** over the same time interval.

1.7.6 Figure 5

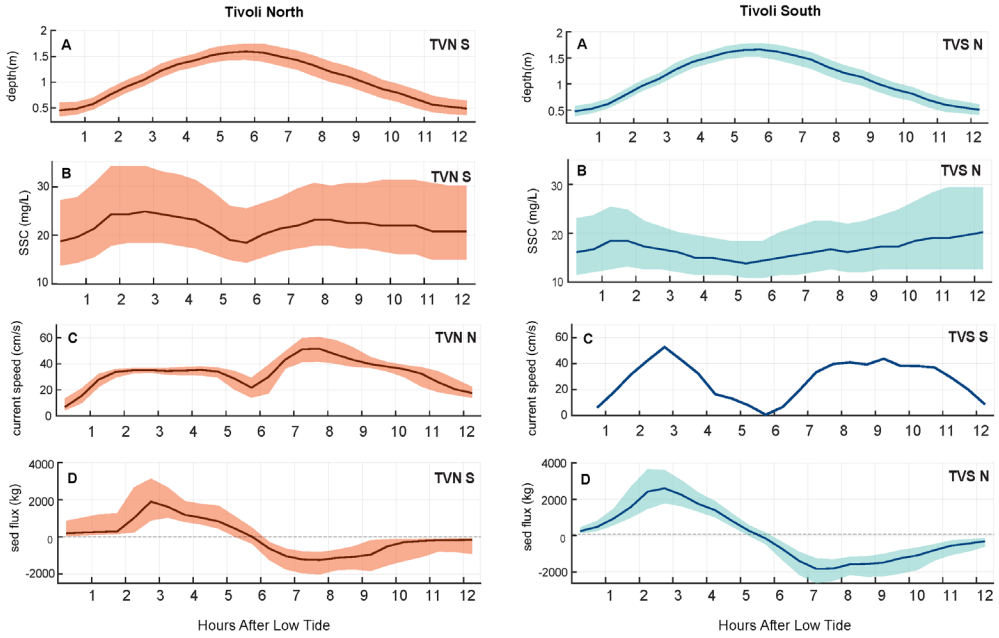

Figure 5. For all panels, medians are shown in solid lines and shading boundaries represent the 25th to 75th percentiles of all tidal cycles from 2004-2019. Tivoli North (TVN) panels are on the left in red, Tivoli South (TVS) panels are on the right in blue. **(A)** Depth (NAVD88) measured by HRNERR long-term monitoring stations. **(B)** HRNERR calculated SSC (mg/L). **(C)** Current speed (cm/s) at the northern culvert in Tivoli North and the southern culvert in Tivoli South, as measured by Lowell Instruments TC-4 Tiltmeters from June-October 2020. Due to sensor failure, only 3 days of data were collected at Tivoli South. **(D)** Calculated sediment flux (kg) at railroad culverts in Tivoli North and Tivoli South based on methods discussed in Section 4.3.

1.7.7 Figure 6

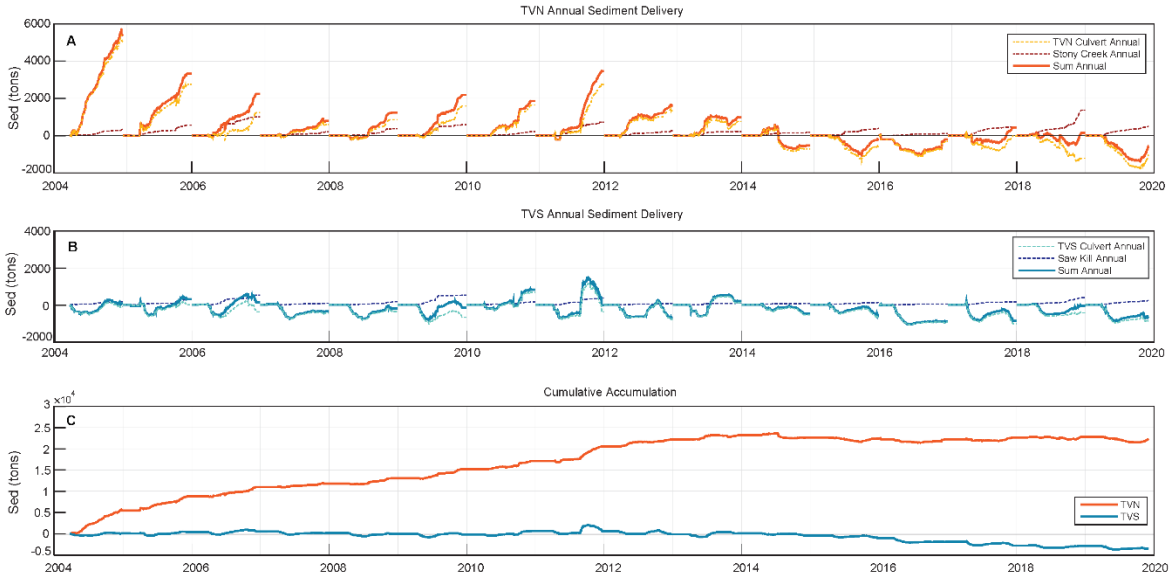

Figure 6. (A) Cumulative sediment fluxes (metric tons) in Tivoli North (TVN) summed annually. Sediment flux at the HRNERR monitored culvert is shown in dashed yellow. Sediment inputs from Stony Creek are shown in dashed red. The sum of these two lines is shown as solid orange. **(B)** Cumulative sediment fluxes in Tivoli South (TVS) summed annually. Sediment flux at the HRNERR monitored culvert is shown in dashed light blue. Sediment inputs from Saw Kill are shown in dashed dark blue. The sum of these two lines is shown as solid blue. **(C)** Cumulative sums of all sediment fluxes in TVN (orange) and TVS (blue) over the study period from 2004-2019.

1.7.8 Figure 7

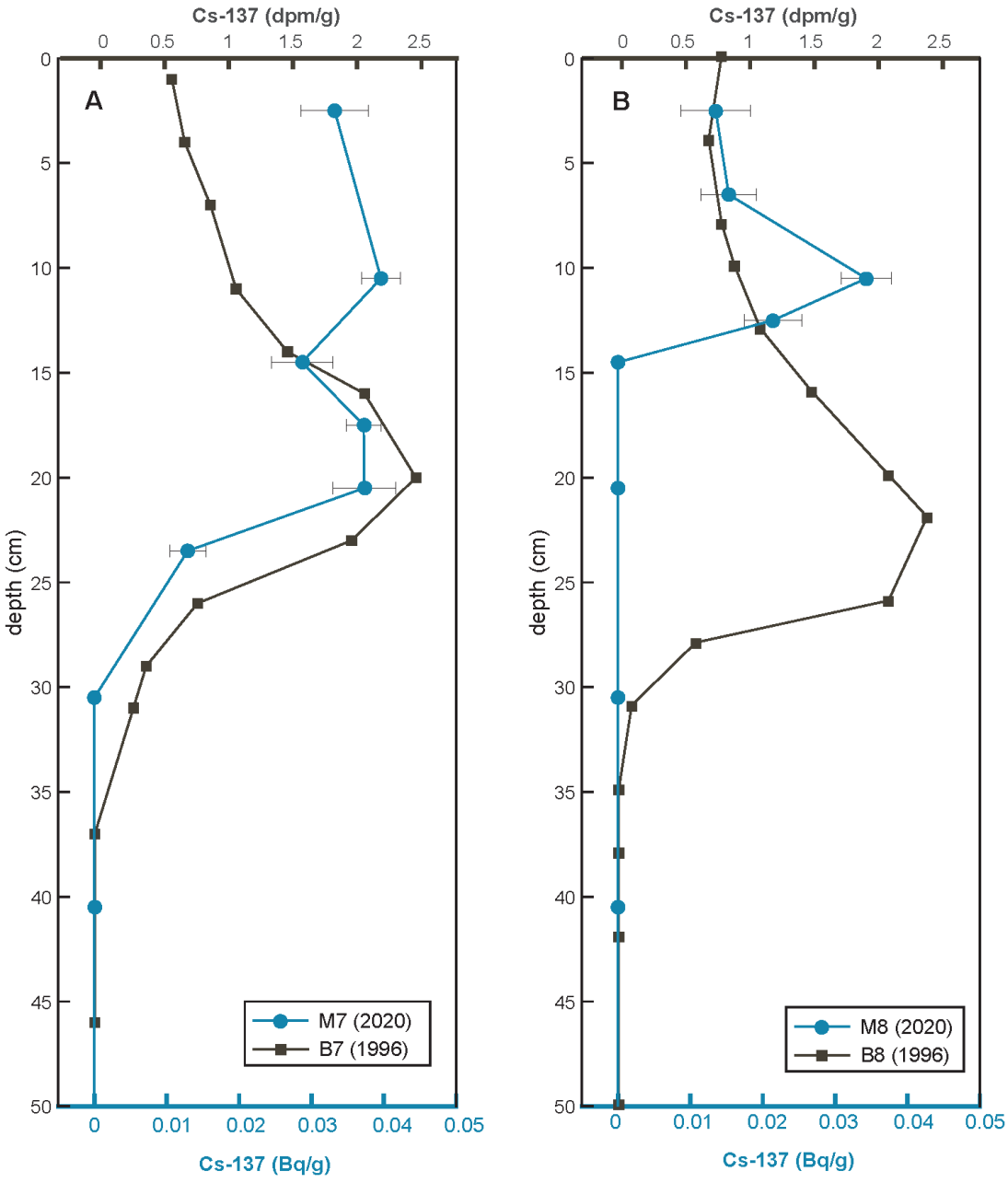

Figure 7. ^{137}Cs profiles from sediment cores M7 **(A)** and M8 **(B)** in blue, with previously published ^{137}Cs profiles from sediment cores B7 and B8 (Benoit et al., 1999) in black.

1.7.9 Figure 8

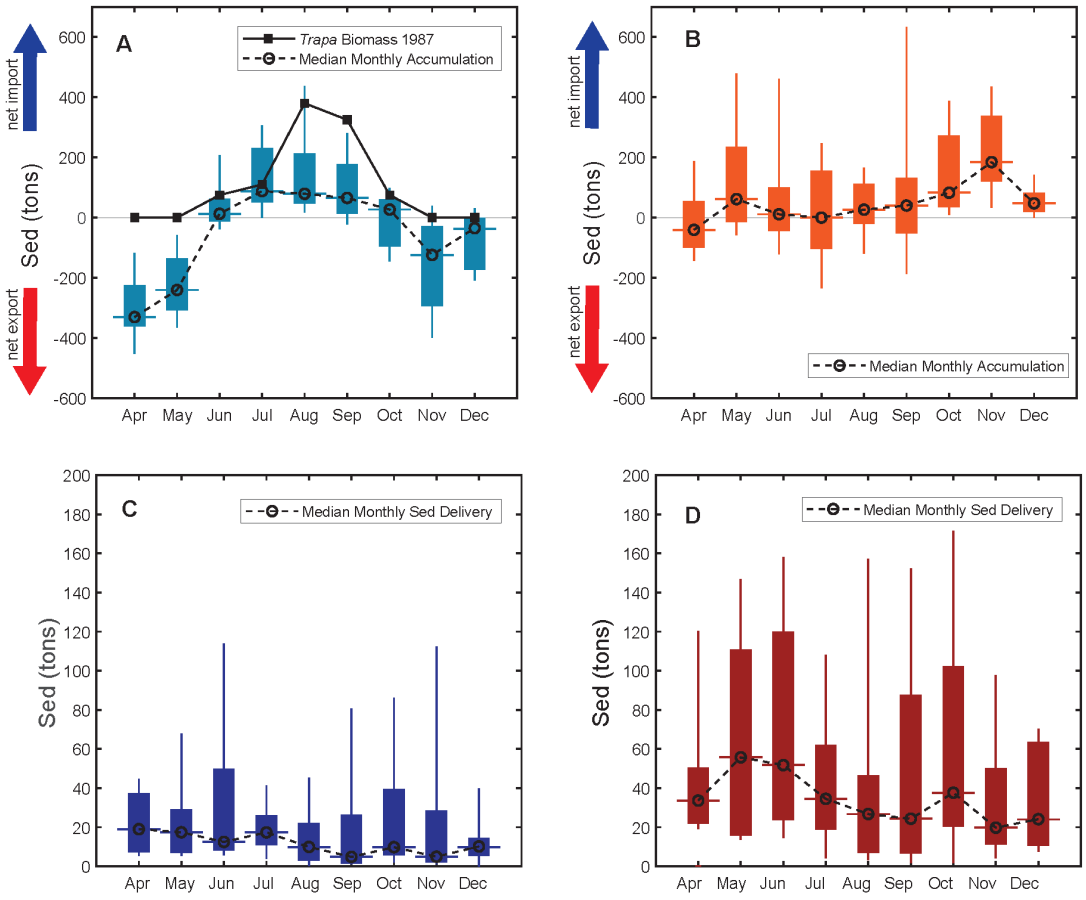

Figure 8. Panels depict 16 years of monthly sediment balances from 2004-2019 at the Tivoli Bays' culverts (top row) and tributaries (bottom row). Boxes encompass the 25th to 75th percentiles, with vertical whiskers spanning the 10th to 90th percentiles and medians marked with a horizontal line. Dashed black lines connect medians marked by open circles. **(A)** Monthly sediment balances at Tivoli South. Biomass of water chestnut in 1987 is shown in black squares (Findlay et al., 1990) **(B)** Monthly sediment balances at Tivoli North. **(C)** Monthly sediment delivery to Tivoli South from the Saw Kill. **(D)** Monthly sediment delivery to Tivoli North from Stony Creek.

CHAPTER 1 REFERENCES

Aggarwala, R. 1993. The Hudson River Railroad and the Development of Irvington, New York, 1849-1860. In: The Hudson Valley Regional Review, pp. 51–80.

Anderson, F.E. and Black, L. 1981. A temporal and spatial study of mudflat erosion and deposition. Journal of Sedimentary Petrology. 51(3): 0729-0736. https://doi.org/10.1306/212F7D8D-2B24-11D7-8648000102C1865D.

Anderson, T.J. 2001. Seasonal variation in erodibility of two temperate, microtidal mudflats. Estuarine, Coastal, and Shelf Science. 53: 1-12. https://doi.org/10.1006/ecss.2001.0790.

Appleby, P.G. 2001. Chronostratigraphic techniques in sediments. In: Tracking Environmental Change Using Lake Sediments. Developments in Paleoenvironmental Research, vol 1. Springer, Dordrecht. pp 171-203. https://doi-org /10.1007/0-306-47669-X_9

Arrigoni, A., Findaly, S., Fischer, D., Tockner, K. 2008. Predicting Carbon and Nutrient Transformations in Tidal Freshwater Wetlands of the Hudson River. Ecosystems. 11: 790-802. https://doi.org/10.1007/s10021-008-9161-0

Baldwin, A.H., 2004. Restoring complex vegetation in urban settings: the case of tidal freshwater marshes. Urban Ecosystems. 7: 125-137. https://doi.org/10.1023/B:UECO.0000036265.86125.34

Baldwin, A.H., Hammerschlag, R.S., Cahoon, D.R. 2019. Chapter 25 – Evaluating restored tidal freshwater wetlands. In: Coastal Wetlands (Second Edition). Elseveir. pp 889-912. https://doi.org/10.1016/B978-0-444-63893-9.00025-3

Barbier, E.B., S.D. Hacker, C. Kennedy, E.W. Koch, A.C. Stier, B.R. Silliman. 2011. The value of estuarine and coastal ecosystem services. Ecological monographs. 81(2):169-193. https://doi.org/10.1890/10-1510.1

Barendregt, A., Whigham, D.F., Meire, P., Baldwin, A.H., Van Damme, S. 2006. Wetlands in the Tidal Freshwater Zone. In: Wetlands: Functioning, Biodiversity Conservation, and Restoration. Ecological Studies (Analysis and Synthesis), vol 191. Springer, Berlin, Heidelberg. https://doi.org/10.1007/978-3-540-33189-6_6

Beauchard, O., Jacobs, S., Cox, T.J.S., Maris, T., Vrebos, D., Braeckel, A.V., Meire, P. 2011. A new technique for tidal habitat restoration: Evaluation of its hydrological potentials. Ecological Engineering. 37: 1849-1858. https://doi.org/10.1016/j.ecoleng.2011.06.010

Beckett, L.H., Baldwin, A.H., Kearney, M.S. 2016. Tidal marshes across a Chesapeake Bay subestuary are not keeping up with sea-level rise. PLoS ONE. 11(7): e0159753. https://doi.org/10.1371.journal.pone.0159753

Benoit, G., Wang, E.X., Nieder, W.C., Levandowsky, M., Breslin, V.T. 1999. Sources and history of heavy metal contamination and sediment deposition in Tivoli South Bay, Hudson River, New York. Estuaries. 22: 167–178. https://doi.org/10.2307/1352974

Boon, J. D. 1975. Tidal discharge asymmetry in a salt marsh drainage system. Limnology and Oceanography. 20: 71-80. https://doi.org/10.4319/lo.1975.20.1.0071

Bowen, M.M., and Geyer, W.R. 2003. Salt transport and the time-dependent salt balance of a partially stratified estuary. Journal of Geophysical Research: Oceans. 108: 3158. https://doi.org/10.1029/2001JC001231

Broome, S.W., Craft, C.B., Burchell, M.R. 2019. Chapter 22 - Tidal Marsh Creation. In: Coastal Wetlands. Elsevier. pp. 789–816. https://doi.org/10.1016/B978-0-444-63893-9.00022-8

Bruegel, M. 2002. Farm, Shop, Landing: The Rise of a Market Society in the Hudson Valley, 1780–1860. Duke University Press.

Butzeck, C., Eschenbach, A., Gröngröft, A., Hansen, K., Nolte, S., Jensen, K. 2015. Sediment deposition and accretion rates in tidal marshes are highly variable along estuarine salinity and flooding gradients. Estuaries and Coasts. 38: 434–450. https://doi.org/10.1007/s12237-014-9848-8

Collins, M.J., Miller, D., 2012. Upper Hudson River Estuary (USA) Floodplain change over the 20th century. River Research and Applications. 28: 1246–1253. https://doi.org/10.1002/rra.1509

Crooks, J.A. 2002. Characterizing ecosystem-level consequences of biological invasions: the role of ecosystem engineers. Oikos 97: 153–166. https://doi.org/10.1034/j.1600-0706.2002.970201.x

Darke, A.K. and Megonigal, J.P. 2003. Controls of sediment deposition rates in two mid-Atlantic tidal freshwater wetlands. Estuarine, Coastal and Shelf Science. 57: 255-268. https://doi.org/10.1016/S0272-7714(02)00353-0

Fagherazzi, S. 2013. The ephemeral life of a salt marsh. Geology. 41(8): 943–944. https://doi.org/10.1130/focus082013.1

Ferrari, M.O., L. Ranåker, K. Weinersmith, M. Young, A. Sih, J.L. Conrad. 2014. Effects of turbidity and an invasive waterweed on predation by introduced largemouth bass. Environmental Biology of Fishes 97: 79–90. https://doi.org/10.1007/s10641-013-0125-7

Findlay, S., Howe, K., Austin, H.K. 1990. Comparison of detritus dynamics in two tidal freshwater wetlands. Ecology 71: 288–295. https://doi.org/10.2307/1940268

Ganju, K.J., Kirwan, M.L., Dickhudt, P.L., Guntenspergen, G.R, Cahoon, D.R., Kroeger, K.D. 2015. Sediment transport-based metrics of wetland stability. Geophysical Research Letters. 45(19): 7992-8000. https://doi.org/10.1002/2015GL065980

Ganju, N.K. 2019. Marshes are the new beaches: Integrating sediment transport into restoration planning. *Estuaries and Coasts.* 42: 917–926. https://doi.org/10.1007/s12237-019-00531-3

Gedan, K.B., Kirwan, M.L., Wolanski, E., Barbier, E.B., Silliman, B.R. 2011. The present and future role of coastal wetland vegetation in protecting shorelines: answering recent challenges to the paradigm. Climatic Change. 106: 7–29. https://doi.org/10.1007/s10584-010-0003-7

Geyer, R.W., Chant, R. 2006. The Physical Oceanography Processes in the Hudson River Estuary. In: The Hudson River Estuary. Cambridge University Press. pp 24-37.

Hestir, E.L., Schoellhamer, D.H., Greenberg, J., Morgan-King, T., Ustin, S.L. 2016. The effect of submerged aquatic vegetation expansion on a declining turbidity trend in the Sacramento-San Joaquin River Delta. Estuaries and Coasts. 39: 1100–1112. https://doi.org/10.1007/s12237-015-0055-z

Horton, R., Little, C., Gornitz, V., Bader, D., Oppenheimer, M. 2015. New York City Panel on Climate Change 2015 Report Chapter 2: Sea Level Rise and Coastal Storms. Annals of the NY Academy of Sciences. 1336(1): 36–44. https://doi.org/10.1111/nyas.12593

Howes, N., FitzGerald, D., Hughes, Z., Georgiou, I., Kulp, M., Miner, M., Smith, J., Barras, J., Thomas, D. 2010. Hurricane-induced failure of low salinity wetlands. PNAS. 107:14014-14019. https://doi.org/10.1073/pnas.0914582107

Hummel, M. and Kiviat, E. 2004. Review of world literature on water chestnut with implications for management in North America. Journal of Aquatic Plant Management. 42: 17–28.

Hummel, M., Findlay, S. 2006. Effects of water chestnut (*Trapa natans*) beds on water chemistry in the tidal freshwater Hudson River. Hydrobiologia. 559: 169–181. https://doi.org/10.1007/s10750-005-9201-0

HRECRP. 2016. Hudson-Raritan Estuary Comprehensive Restoration Plan. NY/NJ Port Auth. and US Army Corps of Engineers. https://www.hudsonriver.org/wp-content/uploads/2017/08/Hudson-raritan-0616.pdf

HRCRP. 2018. Hudson River Comprehensive Restoration Plan. Hudson River Shorelines and Riparian Areas Team. http://thehudsonweshare.org/wp-content/uploads/2018/08/Hudson-River-Shorelines-and-Riparian-Areas.pdf

Kemp, A.C., Hill, T.D., Vane, C.H., Cahill, N., Orton, P.M., Talke, S.A., Parnell, A.C., Sanborn, K., Hartig, E.K. 2017. Relative sea-level trends in New York City during the past 1500 years. The Holocene. 27: 1169–1186. https://doi.org/10.1177/0959683616683263

Kirwan, M.L., Murray, A.B., Donnelly, J.P., Corbett, D.R., 2011. Rapid wetland expansion during European settlement and its implication for marsh survival under modern sediment delivery rates. Geology. 39: 507–510. https://doi.org/10.1130/G31789.1

Kiviat, E., Findlay, S.E.G, Nieder, W.C. 2006. Tidal wetlands of the Hudson River Estuary. In: The Hudson River Estuary. Cambridge University Press. pp 279-295.

Knutson, P.L., Brochu, R.A., Seelig, W.N., Inskeep, M. 1982. Wave damping in Spartina alterniflora marshes. Wetlands. 2: 87–104. https://doi.org/10.1007/BF03160548

Kopp, R.E. 2013. Does the mid-Atlantic United States sea level acceleration hot spot reflect ocean dynamic variability? Geophysical Research Letters. 40: 3981–3985. https://doi.org/10.1002/grl.50781

Loomis, M.J., Craft, B.C. 2010. Carbon sequestration and nutrient (nitrogen, phosphorous) accumulation in river-dominated tidal marshes, Georgia, USA. Wetland Soils. 74(3): 1028-1036. https://doi.org/10.2136/sssaj2009.0171

Lumia, R. Freehafer, D.A., Smith, M.J. 2006. Magnitude and frequency of floods in New York: U.S. Geological Survey Scientific Investigations Report 2006–5112, 152 p.

Madsen, J.D., P.A. Chambers, W.F. James, E.W. Koch, and D.F. Westlake. 2001. The interaction between water movement, sediment dynamics and submersed macrophytes. Hydrobiologia 44: 71–84. https://doi.org/10.1023/A:1017520800568

Marcus, W. A., Kearney, M.S. 1991. Upland and coastal sediment sources in a Chesapeake Bay Estuary. Annals of the Association of American Geographers. 81(3): 408-424. https://doi.org/10.1111/j.1467-8306.1991.tb01702.x

Merrill, J.Z., Cornwell, J.C. 2002. The role of oligohaline marshes in estuarine nutrient cycling. In: Concepts and Controversies in Tidal Marsh Ecology. Springer, Dordrecht. https://doi.org/10.1007/0-306-47534-0_19

Miller, D., Ladd, J., Nieder, W.C., 2006. Channel morphology in the Hudson River Estuary: Historical changes and opportunities for restoration. In: American Fisheries Society Symposium. American Fisheries Society. p 29.

Minello, T.J., Rozas, L.P., Baker, R. 2012. Geographic variability in salt marsh flooding patterns may affect nursery value for fishery species. Estuaries and Coasts. 35: 501–514. https://doi.org/10.1007/s12237-011-9463-x

Mitsch, W.J., Gosselink, J.G., 2000. Wetlands in the tidal freshwater zone. In: Wetlands: Functioning, Biodiversity Conservation, and Restoration. Springer-Verlag, Berlin. pp 117-148.

Nardin, W., Edmonds, D.A., Fagherazzi, S. 2016. Influence of vegetation on spatial patterns of sediment deposition in deltaic islands during flood. Advances in Water Resources. 93: 236-248. https://doi.org/10.1016/j.advwatres.2016.01.001

Naylor, M. 2003. Water Chestnut (*Trapa natans*) in the Chesapeake Bay Watershed: A Regional Management Plan. Maryland Department of Natural Resources. https://www.fws.gov/anstaskforce/Species%20plans/Water%20Chestnut%20Mgt%20Plan.pdf

NFWF. 2014. National Fish and Wildlife Foundation. 2014 Conservation investments. http://www.nfwf.org/whoweare/mediacenter/Documents/2014-nfwf-grants-list.pdf. Accessed 7 April 2021.

Neubauer, S. C., Anderson, I. C., Constantine, J. A., Kuehl, S. A. 2002. Sediment deposition and accretion in a Mid-Atlantic (U.S.A) Tidal Freshwater Marsh. Estuarine, Coastal, and Shelf Science. 54: 713-727. https://doi.org/10.1006/ecss.2001.0854

Neubauer, S. C. 2008. Contributions of mineral and organic components to tidal freshwater marsh accretion. Estuarine, Coastal and Shelf Science. 78: 78-88. https://doi.org/10.1016/j.ecss.2007.11.011

NOAA. 2014. 2013 USGS Lidar: NY post-Sandy, Ulster, Dutchess, Orange Counties. Charleston, South Carolina: Office for Coastal Management.

NYSIS. 2019. New York State Invasive Species Information, Water Chestnut. http://nyis.info/invasive_species/water-chestnut/

Odum, W.E., 1988. Comparative ecology of tidal freshwater and salt marshes. Annual Review of Ecology and Systematics. 19: 147-176.

Pasternack, G.B. and Brush, G.S. 2001. Seasonal variations in sedimentation and organic content in five plant associations on a Chesapeake Bay tidal freshwater delta. Estuarine, Coastal and Shelf Science. 53: 93-106. https://doi.org/10.1006/ecss.2001.0791

Ralston, D.K., Geyer, W.R., and Lerczak. J.A. 2008. Subtidal salinity and velocity in the Hudson River Estuary: Observations and modeling. Journal of Physical Oceanography. 38: 753–887. https://doi.org/10.1175/2007JPO3808.1

Ralston, D.K., Geyer, W.R. 2009. Episodic and long-term sediment transport capacity in the Hudson River Estuary. Estuaries and Coasts. 32: 1130. https://doi.org/10.1007/s12237-009-9206-4

Ralston, D.K., Talke, S., Geyer, W.R., Al-Zubaidi, H.A., Sommerfield, C.K., 2019. Bigger tides, less flooding: Effects of dredging on barotropic dynamics in a highly modified estuary. Journal of Geophysical Research: Oceans. 124: 196–211. https://doi.org/10.1029/2018JC014313

Ralston, D.K., Yellen, B., Woodruff, J.D. 2021. Watershed suspended sediment supply and potential impacts of dam removals for an estuary. Estuaries and Coasts. https://doi.org/10.1007/s12237-020-00873-3

Reed, D., van Wesenbeeck, B., Herman, P.M., and Meselhe, E. 2018. Tidal flat-wetland systems as flood defenses: Understanding biogeomorphic controls. Estuarine, Coastal and Shelf Science. 213: 269–282. https://doi.org/10.1016/j.ecss.2018.08.017

Schoellhamer, D.H., S.A. Wright, and J.Z. Drexler. 2012. A conceptual model of sedimentation in the Sacramento-San Joaquin Delta. San Francisco Estuary and Watershed Science. 10(3). https://doi.org/10.15447/sfews.2012v10iss3art3

Spencer, T., Schuerch, M., Nicholls, R.J., Hinkel, J., Lincke, D., Vafeidis, A.T., Reef, R., McFadden, L., Brown, S. 2016. Global coastal wetland change under sea-level rise and related stresses: The DIVA Wetland Change Model. Global and Planetary Change. 139: 15–30. https://doi.org/10.1016/j.gloplacha.2015.12.018

Squires, D.F., 1992. Quantifying anthropogenic shoreline modification of the Hudson River and Estuary from European contact to modern time. Coastal Management. 20: 343–354. https://doi.org/10.1080/08920759209362183

Sritrairat, S., Peteet, D.M., Kenna, T.C., Sambrotto, R., Kurdyla, D., Guilderson, T. 2012. A history of vegetation, sediment and nutrient dynamics at Tivoli North Bay, Hudson Estuary, New York. Estuarine, Coastal and Shelf Science. 102–103: 24–35. https://doi.org/10.1016/j.ecss.2012.03.003

Strayer, D.L. 2010. Alien species in fresh waters: ecological effects, interactions with other stressors, and prospects for the future. Freshwater Biology. 55(1): 152-174. https://doi.org/10.1111/j.1365-2427.2009.02380.x

Tabak, N.M., Laba, M., Spector, S. 2016. Simulating the effects of sea level rise on the resilience and migration of tidal wetlands along the Hudson River. PLoS ONE. 11(4): e0152437. https://doi:10.1371/journal.pone.0152437

Temmerman, S., Govers, G., Wartel, S., Meire, P. 2003. Spatial and temporal factors controlling short-term sedimentation in a salt and freshwater tidal marsh, Scheldt Estuary, Belgium, SW Netherlands. Earth Surface Processes and Landforms. 28:739-755. https://doi.org/10.1002/esp.495

US Census Bureau. 2011. Population Distribution and Change: 2000 to 2010. 2010 Census Briefs. https://www.census.gov/prod/cen2010/briefs/c2010br-01.pdf

USGS. 2016. The StreamStats program. Online at http://streamstats.usgs.gov, accessed on May 4, 2020.

Wall, G.R., Nystrom, E.A. and Litten, S. 2008. Suspended sediment transport in the freshwater reach of the Hudson River Estuary in Eastern New York. Estuaries and Coasts. 31: 542–553. https://doi.org/10.1007/s12237-008-9050-y

Whigham, D.F., Baldwin, A.H., Barendregt, A. 2009. Tidal freshwater wetlands. In: Coastal wetlands: an integrated ecosystem approach. Elsevier, Amsterdam. pp 515-534.

Work, P.A., Downing-Kunz, M., Drexler, J.Z. 2021. Trapping of suspended sediment by submerged aquatic vegetation in a tidal freshwater region: field observations and long-term trends. Estuaries and Coast. 44: 734-749. https://doi.org/10.1007/s12237-020-00799-w

Yellen, B., Woodruff. J.D., Ladlow, C., Ralston, D.K., Fernald, S., Lau, W. 2020. Rapid tidal marsh development in anthropogenic backwaters. Earth Surf. Process. Landforms. 2021; 1–20. https://doi.org/10.1002/esp.5045

CHAPTER 2

SUPPLEMENTAL MATERIAL

2.1 Study Site (Supplemental)

2.1.1 Anthropogenic Modifications to the Estuary

The Hudson River Estuary has been impacted by Indigenous humans for thousands of years, and the arrival of white colonists in the 1600's more severely altered the landscape via settlement construction and destruction, hunting, trapping, logging, and farming. As populations in New York State grew and capitalist economies expanded upriver, the industrial development of the 1800s further modified the river and its watershed area in more significant ways (Bruegel, 2002; Kurlansky, 2006). The onset of industrialization saw extensive mill construction, resulting in substantial damming of both the Hudson River and its tributaries. Widespread and thorough deforestation along the upper Hudson's steep shorelines coincided with this mill construction, causing considerable erosion and potentially enhanced sediment delivery to the river (Hilfinger IV et al., 2001; Kudish, 2000; Wahlen and Lewis, 1980). However, recent studies indicate that many dams on the Hudson are scarcely impounding sediment, and downstream environmental effects are minimal (Ralston et al., 2021). It remains unclear to what extent the increased erosion from deforestation has affected sediment load and delivery to the estuary, although precipitation and flood frequency in this area have largely increased with climate change, which may be accelerating erosion and increasing sediment yields (Armstrong et al., 2012, Cook et al., 2015, Yellen and Steinschneider, 2019).

In 1831, the US Army Corps of Engineers constructed various dikes that constricted flow to a single channel and increased scour to deepen the main channel of the Hudson River (Collins and Miller, 2012; Miller et al., 2006). Alongside supplemental dredging, these federal navigation projects transformed the shallow braided river channel of the upper Hudson (river km 190 – 240) to a single deep, fast-flowing channel that enabled the safe passage of large vessels from New York City to Albany, and on to the Erie Canal (Collins and Miller, 2012). In 1819 the average channel depth in the upper Hudson was ~ 1 m. Dredging projects increased the average channel depth to 9.7 m by the 1930s, with much of the navigation channel within the tidal reach ranging between 10 and 20 m depth (Collins and Miller, 2012, Yellen et al., 2020). This dredging and deepening reduced effective drag and increased drainage efficiency, resulting in an increased tidal range and amplified tides in the upper Hudson, while decreasing mean water level of the estuary (Ralston et al., 2019).

2.2 Methods (Supplemental)

2.2.1 Water Column Observations

When depth or turbidity values were flagged as anomalous by the HRNERR quality control system, they were coded as null values in the water column flux calculations. When null values appeared in the depth timeseries, the previous and subsequent time steps were used as the temporal boundaries to determine change in water depth, volume, and ultimately flux, over the time period containing the null value. When turbidity measurements were excluded due to instrument malfunction, the SSC

value for that time step was not extrapolated within the interpolation. If either a depth or turbidity value was excluded due to quality control flags, sediment flux was not calculated at that time step, and sediment loss or accumulation over the missing period was inferred in the same way as water flux described above. Cumulative sediment amount remained constant during time periods with missing values and the Q_s of the subsequent time step was added to the cumulative total at the previous time step, regardless of the amount of time spanning the null values.

In addition to the long-term monitoring stations maintained by HRNERR at the Tivoli North Southern Culvert and the Tivoli South Northern Culvert, we deployed HOBO water level loggers from July 21 to October 19, 2020, at both culverts in Tivoli North, the northern and southernmost culverts in Tivoli South, and in two locations on the marsh platform in Tivoli North (Figure 1). Due to equipment malfunction, the sensor at the Tivoli South northern culvert was removed on August 19, 2020. These water depth loggers collected data at 15-minute resolution and were surveyed in using RTK point elevation measurements tied into the NAVD88 datum to allow for direct comparison to lidar elevations and publicly available depth measurements. At the 15-minute resolution, no significant difference was observed between the time-series of depths at different culverts in the same bay (data available at UMass Scholarworks). Due to standardized culvert size (~25 m across) and the observed consistent water depths across culverts tidal water flux was assumed to be equivalent at all culverts within a specific bay. To validate these water flux measurements, ADCP surveys were conducted at all culverts on October 19, 2020 over the course of one tidal cycle. The ADCP was

passed between two to five times on the bay side of each culvert over time frames ranging from twenty minutes to one hour, and the averages of these results are compared to averages of depth-derived discharge measurements over the same time periods in Supplemental Figure 7. We found that equation $Q_{tide} = \frac{dh}{dt}A$ predicted discharge on the same order of magnitude as the ADCP and we applied this equation to approximate sediment flux in both bays.

Lowell Instruments TC-4 tiltmeters were deployed in tandem with all HOBO sensors from July 21 to October 19, 2020 to test velocity equivalency between culverts in each bay and validate the assumption of a standing tide system used to make time-varying depth-derived flux approximations (i.e. $Q_{tide} = \frac{dh}{dt}A$). These instruments collected continuous speed and heading data at one minute resolution. The two tiltmeters in Tivoli South were found to have stopped functioning after three days of deployment. The instrument at the southern culvert was repaired and redeployed on August 19, 2020 but was not placed deep enough to capture the low tide, and data from a full tidal cycle could not be obtained. Tiltmeter current data and HOBO data confirmed that slack tide occurs at high and low water and peak flood/ebb flows occur during rising and falling tides, supporting the standing wave assumption underlying our tidal flux calculations (Supplemental Figure 3). Two Mayfly Turbidity sensors were deployed with the water level loggers and tiltmeters at the southern culvert in Tivoli South and the northern culvert in Tivoli North. Unlike the HRNERR turbidity sensors, which are stationed within a protective corral, these sensors were deployed in open water and

quickly became biofouled. The optical sensors seem to have been obscured with debris for most of the data collection period and the data was not utilized.

2.2.2 Turbidity-SSC Calibration

Regressions were also run independently for SC (n = 63) and SK (n = 50) and it was determined that combining the samples into a single turbidity-SSC calibration did not affect the outcome. To test if the turbidity signal was obscured by organic material, samples with clastic fractions below 0.8 were removed from sediment budget calculations (Figure 3). Selecting for just clastic sediments only slightly enhanced the divergence between the accumulation regimes identified in the final sediment budgets, and we chose not to remove the organic components from the sediment budgets.

2.2.3 Elevation Determination

Lidar data (NOAA, 2014) was cross-checked against RTK point elevation measurements from three transects administered by HRNERR in Tivoli North in 2013. We conducted three RTK transects in Tivoli South at low tide in June 2020 to also assess lidar's accuracy in the mudflat. We used the average offset between the RTK and lidar elevations in each bay as a correction factor in our tidal prism calculations (Supplemental Figure 4).

2.2.4 Sediment Core and Trap Processing

Cores were processed at the University of Massachusetts-Amherst where they were split, described, and refrigerated. Split cores were scanned on an ITRAX X-Ray

Fluorescence (XRF) core scanner with a Molybdenum tube at 2 mm resolution, using settings outlined for Hudson River sediments in Yellen et al. (2020). The onset of Zn has been used as a stratigraphic marker in Tivoli (Benoit et al., 1999; Yellen et al., 2020) and other Hudson River locations (Brandon et al., 2014) to identify the onset of the heavy industrialization period in 1850. However, Zn profiles from our sediment cores appeared subjected to significant bioturbation in the upper meter, and XRF data was ultimately excluded from this analysis.

Upon sediment trap retrieval, we were unable to recover traps from Stations 1 and 4 in Transect 1 and believe they may have been pushed out of the sediment by growing vegetation (Figure 1). Sediment traps that had visible algal mats grown over the surface were discarded from the analysis, as were traps that were filled to the surface with sediment. This resulted in six traps excluded from Transect 1 and one trap excluded from Transect 2. Three transects of traps were also deployed at Tivoli South in June but were unable to be recovered due to water chestnut coverage.

2.3 Supplemental Figures

2.3.1 Supplemental Figure 1

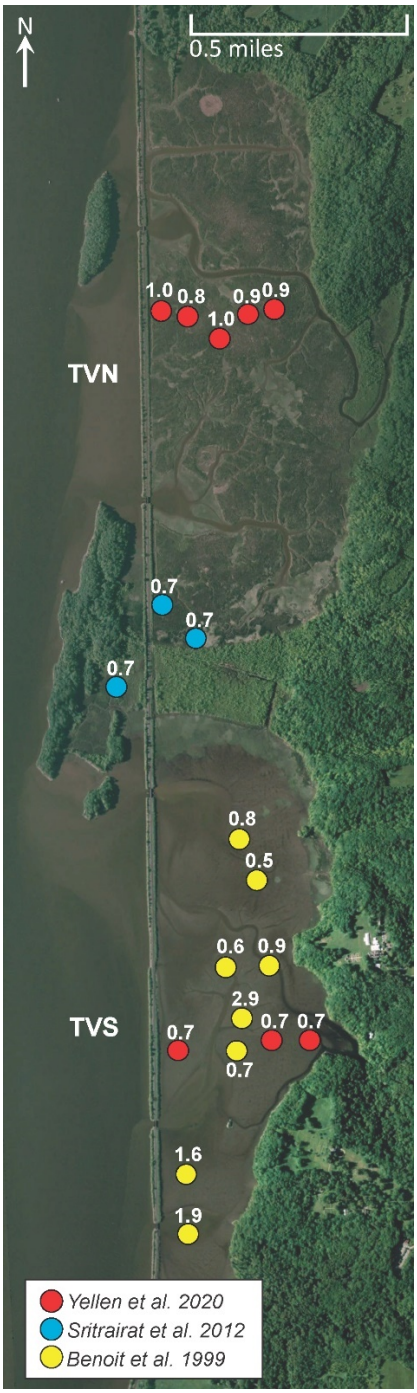

Supplemental Figure 1. Previously published sediment-core based accumulation rates from the Tivoli Bays in cm/yr.

2.3.2 Supplemental Figure 2

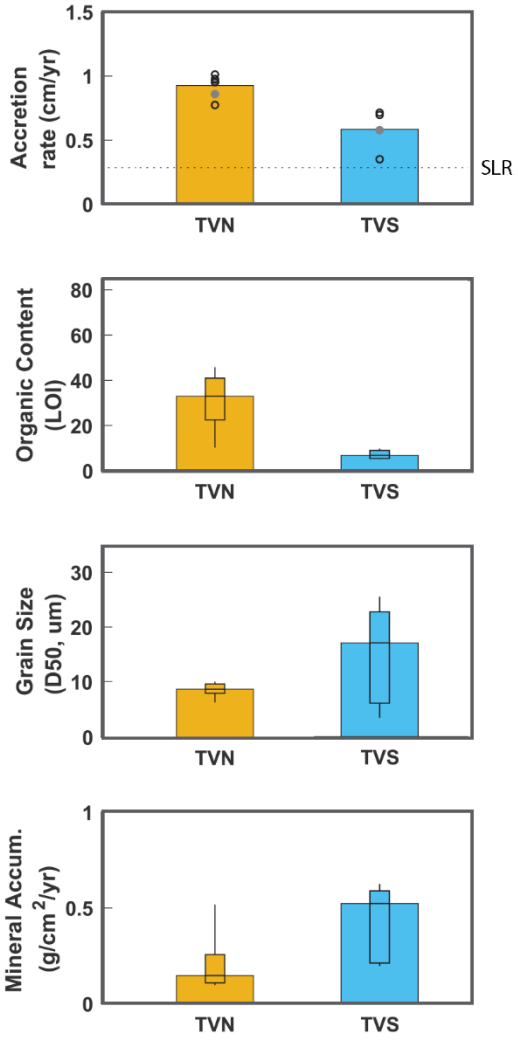

Supplemental Figure 2. Modified from Yellen et al. (2020). Data in all panels is based on the upper 50cm of sediment cores. In the top panel, filled grey and black circles symbolize the potential spread of accumulation rates based on various stratigraphic markers in the age-depth model. In the bottom three plots, the main bar represents the median, with the boundaries of the inset boxes representing the 25th to 75th percentiles and whiskers marking the 10th to 90th percentiles. **(A)** Total accretion rates in the Tivoli Bays with average relative Sea Level Rise (SLR) measured at the Battery, NY (NOAA, Station ID: 8518750) denoted by the dashed line. **(B)** Percent organic content in the Tivoli Bays as determined by Loss-On-Ignition (LOI). **(C)** Grain size in the Tivoli Bays (µm). **(D)** Minerogenic accumulation in the Tivoli Bays (g/cm^2/yr).

2.3.3 Supplemental Figure 3

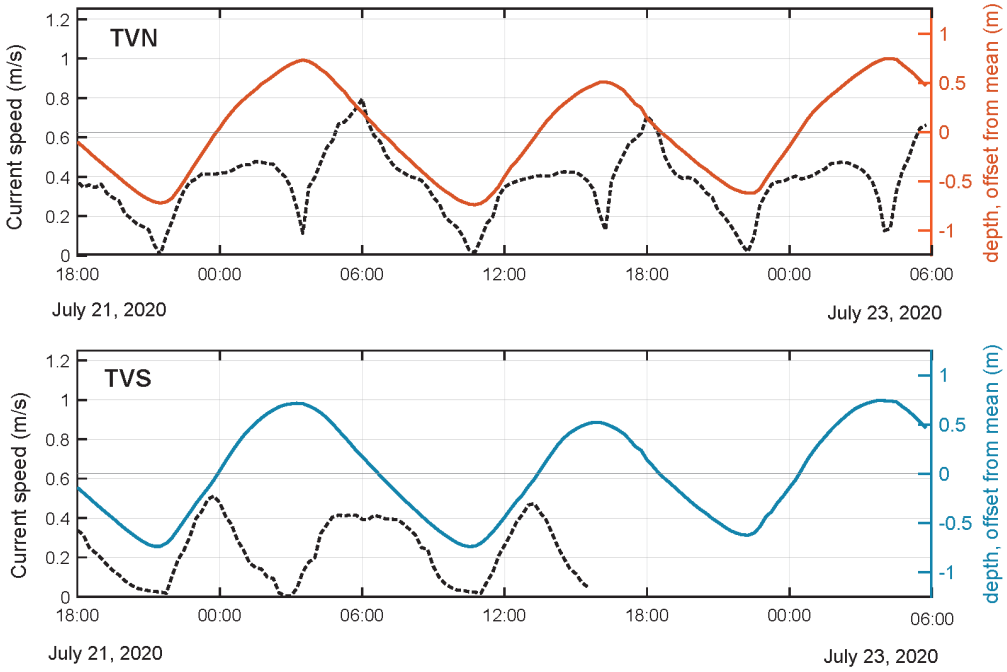

Supplemental Figure 3. Current speed and water level inferred from TCM-4 Tiltmeters and HOBO water level loggers at the southern culvert in Tivoli North (TVN, top) and the northern culvert in Tivoli South (TVS, bottom) in dashed black lines. Water depth (m) from HOBO water level loggers is depicted by solid lines at Tivoli North (TVN, orange) and Tivoli South (TVS, blue). Sensor interference may be responsible for the diminished current peaks on flood and ebb tide in Tivoli North and Tivoli South, respectively.

2.3.4 Supplemental Figure 4

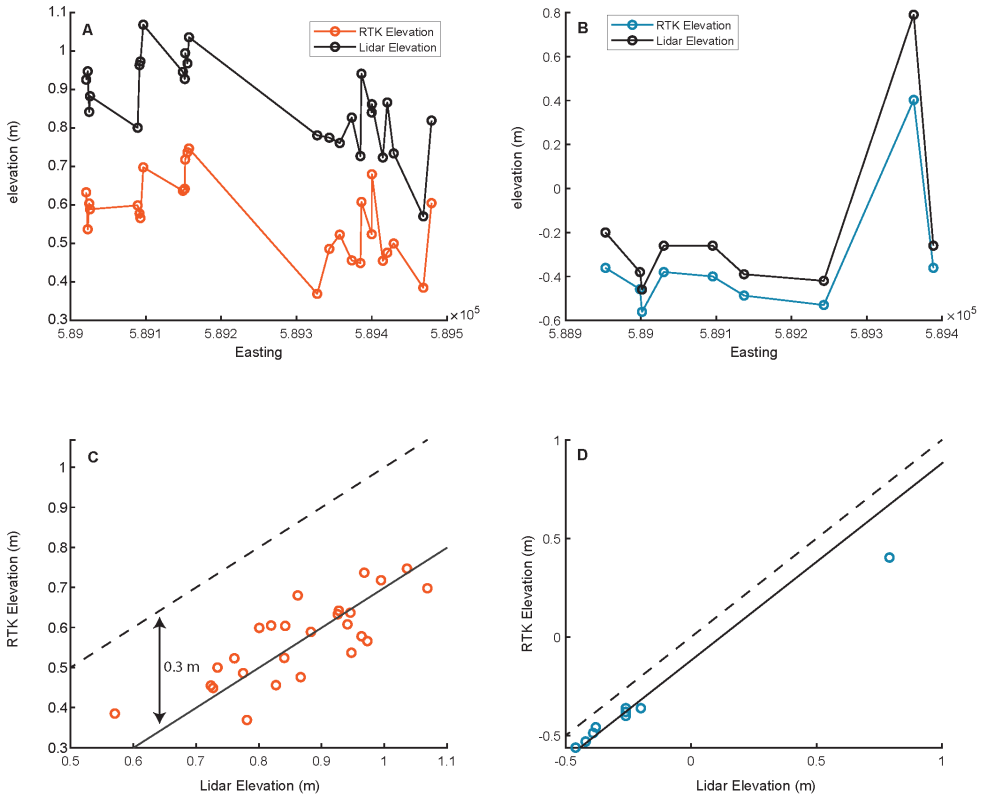

Supplemental Figure 4. (A) Black circles represent elevations of points in Tivoli North determined by a USGS lidar survey conducted in 2014. Orange circles signify elevations determined by a 2013 RTK survey conducted by HRNERR in Tivoli North. (**B)** Black circles represent elevations of points in Tivoli South determined by lidar in 2014. Blue circles indicate elevations determined by a June 2020 RTK survey done for this study. (**C)** Lidar elevation vs RTK elevation in Tivoli North with 1:1 reference line in dashed black and correction factor show in solid black. (**D)** Lidar elevation vs RTK elevation in Tivoli South with 1:1 reference line in dashed black and correction factor in solid black.

2.3.5 Supplemental Figure 5

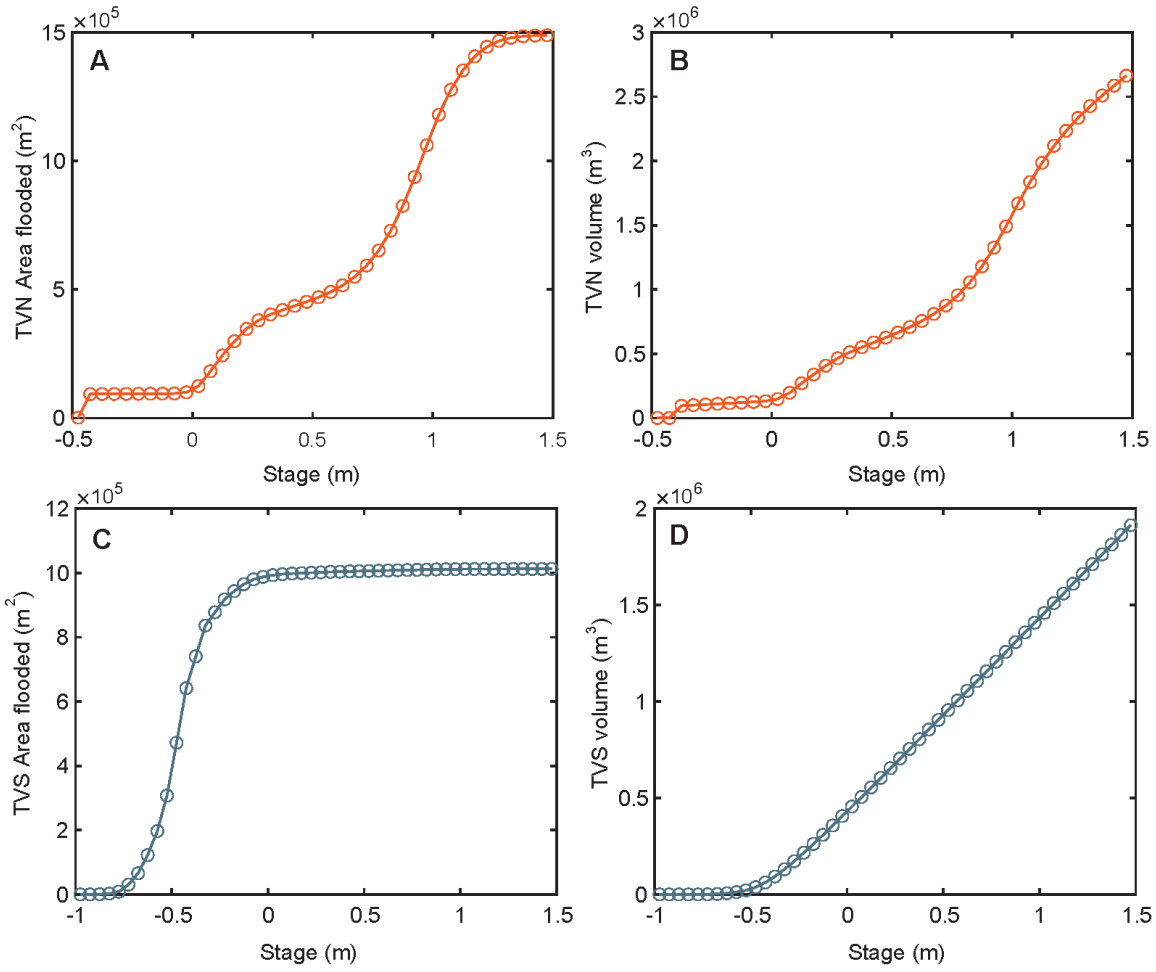

Supplemental Figure 5. Tidal prisms for the Tivoli Bays. **(A)** Tidal stage (m) vs area (m^2) of the marsh platform flooded in Tivoli North (TVN). **(B)** Tidal stage (m) vs volume (m^3) of water in Tivoli North. **(C)** Tidal stage (m) vs area (m^2) of the mudflat flooded in Tivoli South (TVS). **(D)** Tidal stage (m) vs volume (m^3) of water in Tivoli South.

2.3.6 Supplemental Figure 6

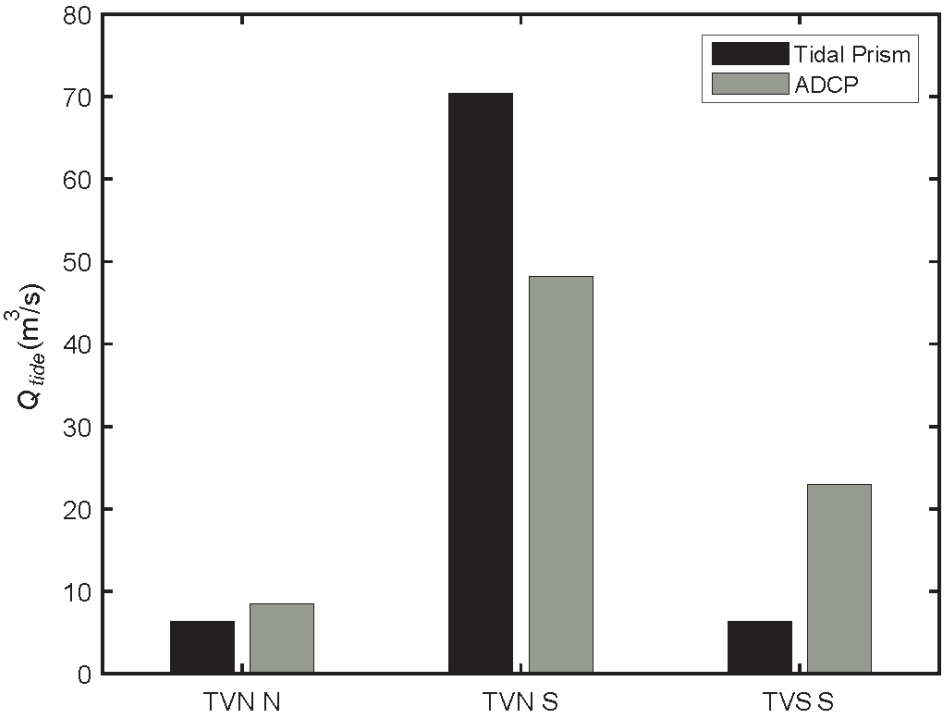

Supplemental Figure 6. Average Q_{tide} (m^3/s) at each culvert measured by ADCP on October 21, 2020 is shown in gray. Average Q_{tide} (m^3/s) at each culvert approximated using the equation $Q_r = \frac{dh}{dt}A$ where h was measured by HOBO dataloggers at 15-minute intervals over the ADCP sampling period is shown in black.

2.3.7 Supplemental Figure 7

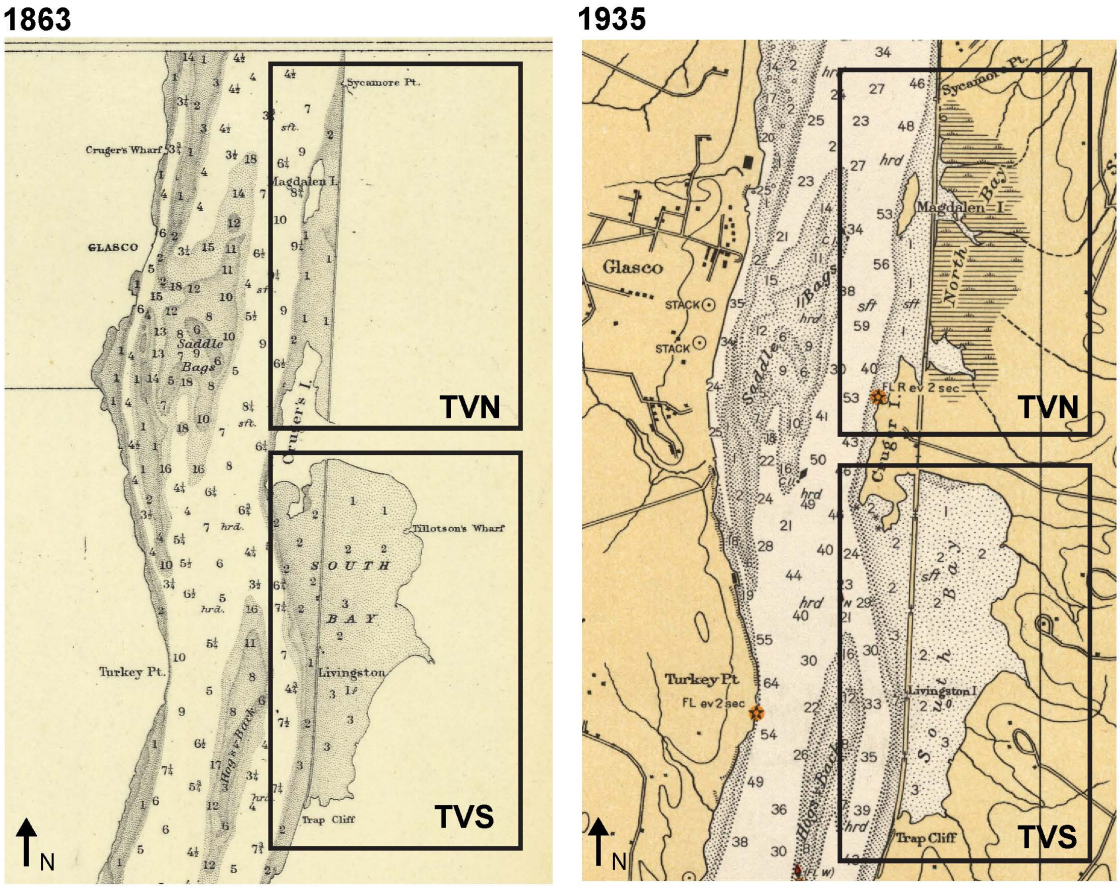

Supplemental Figure 7. Historical charts from 1863 (left) and 1935 (right). (NOAA, https://historicalcharts.noaa.gov).

CHAPTER 2 REFERENCES

Armstrong, W.H., Collins, M.J. & Snyder, N.P. 2012. Increased frequency of low-magnitude floods in New England. JAWRA: Journal of the American Water Resources Association. 48: 306–320. https://doi.org/10.1111/j.1752-1688.2011.00613.x

Brandon, C.M., Woodruff, J.D., Donnelly, J.P., Sullivan, R.M. 2014. How unique was Hurricane Sandy? Sedimentary reconstructions of extreme flooding from New York Harbor. Scientific reports. 4(1): 1–9. https://doi.org/10.1038/srep07366

Bruegel, M. 2002. Farm, Shop, Landing: The Rise of a Market Society in the Hudson Valley, 1780–1860. Duke University Press.

Cook, T.L., Yellen, B.C., Woodruff, J.D., Miller, D. 2015. Contrasting human versus climatic impacts on erosion. Geophysical Research Letters. 42: 6680–6687. https://doi.org/10.1002/2015GL064436

Collins, M.J., Miller, D., 2012. Upper Hudson River Estuary (USA) Floodplain change over the 20th century. River Research and Applications. 28: 1246–1253. https://doi.org/10.1002/rra.1509

Hilfinger IV, M.F., Mullins, H.T., Burnett, A., Kirby, M.E., 2001. A 2500-year sediment record from Fayetteville Green Lake, New York: evidence for anthropogenic impacts and historic isotope shift. Journal of Paleolimnology. 26: 293–305. https://doi.org/10.1023/A:1017560300681

Kudish, M., 2000. The Catskill forest: a history. Purple Mountain Press.

Kurlansky, M. 2006. The Big Oyster: History on the Half Shell. Penguin Random House: New York.

Miller, D., Ladd, J., Nieder, W.C. 2006. Channel morphology in the Hudson River Estuary: Historical changes and opportunities for restoration. In: American Fisheries Society Symposium. American Fisheries Society. p 29.

Ralston, D.K., Talke, S., Geyer, W.R., Al-Zubaidi, H.A., Sommerfield, C.K. 2019. Bigger tides, less flooding: Effects of dredging on barotropic dynamics in a highly modified estuary. Journal of Geophysical Research: Oceans. 124: 196–211. https://doi.org/10.1029/2018JC014313

Ralston, D.K., Yellen, B., Woodruff, J.D. 2021. Watershed suspended sediment supply and potential impacts of dam removals for an estuary. Estuaries and Coasts. https://doi.org/10.1007/s12237-020-00873-3.

Wahlen, M. and Lewis, D.M. 1980. Green Lake: Dating of laminated sediment. EOS Trans. Amer. Geophys. Un. Abs. 61/46: 964.

Yellen, B., Woodruff. J.D., Ladlow, C., Ralston, D.K., Fernald, S., Lau, W. 2020. Rapid tidal marsh development in anthropogenic backwaters. Earth Surf. Process. Landforms. 2021; 1–20. https://doi.org/10.1002/esp.5045

COMBINED BIBLIOGRAPHY

Aggarwala, R. 1993. The Hudson River Railroad and the Development of Irvington, New York, 1849-1860. In: The Hudson Valley Regional Review, pp. 51–80.

Anderson, F.E. and Black, L. 1981. A temporal and spatial study of mudflat erosion and deposition. Journal of Sedimentary Petrology. 51(3): 0729-0736. https://doi.org/10.1306/212F7D8D-2B24-11D7-8648000102C1865D.

Anderson, T.J. 2001. Seasonal variation in erodibility of two temperate, microtidal mudflats. Estuarine, Coastal, and Shelf Science. 53: 1-12. https://doi.org/10.1006/ecss.2001.0790.

Appleby, P.G. 2001. Chronostratigraphic techniques in sediments. In: Tracking Environmental Change Using Lake Sediments. Developments in Paleoenvironmental Research, vol 1. Springer, Dordrecht. pp 171-203. https://doi-org /10.1007/0-306-47669-X_9

Arrigoni, A., Findaly, S., Fischer, D., Tockner, K. 2008. Predicting Carbon and Nutrient Transformations in Tidal Freshwater Wetlands of the Hudson River. Ecosystems. 11: 790-802. https://doi.org/10.1007/s10021-008-9161-0

Armstrong, W.H., Collins, M.J. & Snyder, N.P. 2012. Increased frequency of low-magnitude floods in New England. JAWRA: Journal of the American Water Resources Association. 48: 306–320. https://doi.org/10.1111/j.1752-1688.2011.00613.x

Baldwin, A.H., 2004. Restoring complex vegetation in urban settings: the case of tidal freshwater marshes. Urban Ecosystems. 7: 125-137. https://doi.org/10.1023/B:UECO.0000036265.86125.34

Baldwin, A.H., Hammerschlag, R.S., Cahoon, D.R. 2019. Chapter 25 – Evaluating restored tidal freshwater wetlands. In: Coastal Wetlands (Second Edition). Elseveir. pp 889-912. https://doi.org/10.1016/B978-0-444-63893-9.00025-3

Barbier, E.B., S.D. Hacker, C. Kennedy, E.W. Koch, A.C. Stier, B.R. Silliman. 2011. The value of estuarine and coastal ecosystem services. Ecological monographs. 81(2):169-193. https://doi.org/10.1890/10-1510.1

Barendregt, A., Whigham, D.F., Meire, P., Baldwin, A.H., Van Damme, S. 2006. Wetlands in the Tidal Freshwater Zone. In: Wetlands: Functioning, Biodiversity Conservation, and Restoration. Ecological Studies (Analysis and Synthesis), vol 191. Springer, Berlin, Heidelberg. https://doi.org/10.1007/978-3-540-33189-6_6

Beauchard, O., Jacobs, S., Cox, T.J.S., Maris, T., Vrebos, D., Braeckel, A.V., Meire, P. 2011. A new technique for tidal habitat restoration: Evaluation of its hydrological

potentials. Ecological Engineering. 37: 1849-1858. https://doi.org/10.1016/j.ecoleng.2011.06.010

Beckett, L.H., Baldwin, A.H., Kearney, M.S. 2016. Tidal marshes across a Chesapeake Bay subestuary are not keeping up with sea-level rise. PLoS ONE. 11(7): e0159753. https://doi.org/10.1371.journal.pone.0159753

Benoit, G., Wang, E.X., Nieder, W.C., Levandowsky, M., Breslin, V.T. 1999. Sources and history of heavy metal contamination and sediment deposition in Tivoli South Bay, Hudson River, New York. Estuaries. 22: 167–178. https://doi.org/10.2307/1352974

Boon, J. D. 1975. Tidal discharge asymmetry in a salt marsh drainage system. Limnology and Oceanography. 20: 71-80. https://doi.org/10.4319/lo.1975.20.1.0071

Bowen, M.M., and Geyer, W.R. 2003. Salt transport and the time-dependent salt balance of a partially stratified estuary. Journal of Geophysical Research: Oceans. 108: 3158. https://doi.org/10.1029/2001JC001231

Brandon, C.M., Woodruff, J.D., Donnelly, J.P., Sullivan, R.M. 2014. How unique was Hurricane Sandy? Sedimentary reconstructions of extreme flooding from New York Harbor. Scientific reports. 4(1): 1–9. https://doi.org/10.1038/srep07366

Broome, S.W., Craft, C.B., Burchell, M.R. 2019. Chapter 22 - Tidal Marsh Creation. In: Coastal Wetlands. Elsevier. pp. 789–816. https://doi.org/10.1016/B978-0-444-63893-9.00022-8

Bruegel, M. 2002. Farm, Shop, Landing: The Rise of a Market Society in the Hudson Valley, 1780–1860. Duke University Press.

Butzeck, C., Eschenbach, A., Gröngröft, A., Hansen, K., Nolte, S., Jensen, K. 2015. Sediment deposition and accretion rates in tidal marshes are highly variable along estuarine salinity and flooding gradients. Estuaries and Coasts. 38: 434–450. https://doi.org/10.1007/s12237-014-9848-8

Collins, M.J., Miller, D., 2012. Upper Hudson River Estuary (USA) Floodplain change over the 20th century. River Research and Applications. 28: 1246–1253. https://doi.org/10.1002/rra.1509

Cook, T.L., Yellen, B.C., Woodruff, J.D., Miller, D. 2015. Contrasting human versus climatic impacts on erosion. Geophysical Research Letters. 42: 6680–6687. https://doi.org/10.1002/2015GL064436

Crooks, J.A. 2002. Characterizing ecosystem-level consequences of biological invasions: the role of ecosystem engineers. Oikos 97: 153–166. https://doi.org/10.1034/j.1600-0706.2002.970201.x

Darke, A.K. and Megonigal, J.P. 2003. Controls of sediment deposition rates in two mid-Atlantic tidal freshwater wetlands. Estuarine, Coastal and Shelf Science. 57: 255-268. https://doi.org/10.1016/S0272-7714(02)00353-0

Fagherazzi, S. 2013. The ephemeral life of a salt marsh. Geology. 41(8): 943–944. https://doi.org/10.1130/focus082013.1

Ferrari, M.O., L. Ranåker, K. Weinersmith, M. Young, A. Sih, J.L. Conrad. 2014. Effects of turbidity and an invasive waterweed on predation by introduced largemouth bass. Environmental Biology of Fishes 97: 79–90. https://doi.org/10.1007/s10641-013-0125-7

Findlay, S., Howe, K., Austin, H.K. 1990. Comparison of detritus dynamics in two tidal freshwater wetlands. Ecology 71: 288–295. https://doi.org/10.2307/1940268

Ganju, K.J., Kirwan, M.L., Dickhudt, P.L., Guntenspergen, G.R, Cahoon, D.R., Kroeger, K.D. 2015. Sediment transport-based metrics of wetland stability. Geophysical Research Letters. 45(19): 7992-8000. https://doi.org/10.1002/2015GL065980

Ganju, N.K. 2019. Marshes are the new beaches: Integrating sediment transport into restoration planning. *Estuaries and Coasts.* 42: 917–926. https://doi.org/10.1007/s12237-019-00531-3

Gedan, K.B., Kirwan, M.L., Wolanski, E., Barbier, E.B., Silliman, B.R. 2011. The present and future role of coastal wetland vegetation in protecting shorelines: answering recent challenges to the paradigm. Climatic Change. 106: 7–29. https://doi.org/10.1007/s10584-010-0003-7

Geyer, R.W., Chant, R. 2006. The Physical Oceanography Processes in the Hudson River Estuary. In: The Hudson River Estuary. Cambridge University Press. pp 24-37.

Hestir, E.L., Schoellhamer, D.H., Greenberg, J., Morgan-King, T., Ustin, S.L. 2016. The effect of submerged aquatic vegetation expansion on a declining turbidity trend in the Sacramento-San Joaquin River Delta. Estuaries and Coasts. 39: 1100–1112. https://doi.org/10.1007/s12237-015-0055-z

Hilfinger IV, M.F., Mullins, H.T., Burnett, A., Kirby, M.E., 2001. A 2500-year sediment record from Fayetteville Green Lake, New York: evidence for anthropogenic impacts and historic isotope shift. Journal of Paleolimnology. 26: 293–305. https://doi.org/10.1023/A:1017560300681

Horton, R., Little, C., Gornitz, V., Bader, D., Oppenheimer, M. 2015. New York City Panel on Climate Change 2015 Report Chapter 2: Sea Level Rise and Coastal Storms. Annals of the NY Academy of Sciences. 1336(1): 36–44. https://doi.org/10.1111/nyas.12593

Howes, N., FitzGerald, D., Hughes, Z., Georgiou, I., Kulp, M., Miner, M., Smith, J., Barras, J., Thomas, D. 2010. Hurricane-induced failure of low salinity wetlands. PNAS. 107:14014-14019. https://doi.org/10.1073/pnas.0914582107

Hummel, M. and Kiviat, E. 2004. Review of world literature on water chestnut with implications for management in North America. Journal of Aquatic Plant Management. 42: 17–28.

Hummel, M., Findlay, S. 2006. Effects of water chestnut (*Trapa natans*) beds on water chemistry in the tidal freshwater Hudson River. Hydrobiologia. 559: 169–181. https://doi.org/10.1007/s10750-005-9201-0

HRECRP. 2016. Hudson-Raritan Estuary Comprehensive Restoration Plan. NY/NJ Port Auth. and US Army Corps of Engineers. https://www.hudsonriver.org/wp-content/uploads/2017/08/Hudson-raritan-0616.pdf

HRCRP. 2018. Hudson River Comprehensive Restoration Plan. Hudson River Shorelines and Riparian Areas Team. http://thehudsonweshare.org/wp-content/uploads/2018/08/Hudson-River-Shorelines-and-Riparian-Areas.pdf

Kemp, A.C., Hill, T.D., Vane, C.H., Cahill, N., Orton, P.M., Talke, S.A., Parnell, A.C., Sanborn, K., Hartig, E.K. 2017. Relative sea-level trends in New York City during the past 1500 years. The Holocene. 27: 1169–1186. https://doi.org/10.1177/0959683616683263

Kirwan, M.L., Murray, A.B., Donnelly, J.P., Corbett, D.R., 2011. Rapid wetland expansion during European settlement and its implication for marsh survival under modern sediment delivery rates. Geology. 39: 507–510. https://doi.org/10.1130/G31789.1

Kiviat, E., Findlay, S.E.G, Nieder, W.C. 2006. Tidal wetlands of the Hudson River Estuary. In: The Hudson River Estuary. Cambridge University Press. pp 279-295.

Knutson, P.L., Brochu, R.A., Seelig, W.N., Inskeep, M. 1982. Wave damping in Spartina alterniflora marshes. Wetlands. 2: 87–104. https://doi.org/10.1007/BF03160548

Kopp, R.E. 2013. Does the mid-Atlantic United States sea level acceleration hot spot reflect ocean dynamic variability? Geophysical Research Letters. 40: 3981–3985. https://doi.org/10.1002/grl.50781

Kudish, M., 2000. The Catskill forest: a history. Purple Mountain Press.

Kurlansky, M. 2006. The Big Oyster: History on the Half Shell. Penguin Random House: New York.

Loomis, M.J., Craft, B.C. 2010. Carbon sequestration and nutrient (nitrogen, phosphorous) accumulation in river-dominated tidal marshes, Georgia, USA. Wetland Soils. 74(3): 1028-1036. https://doi.org/10.2136/sssaj2009.0171

Lumia, R. Freehafer, D.A., Smith, M.J. 2006. Magnitude and frequency of floods in New York: U.S. Geological Survey Scientific Investigations Report 2006–5112, 152 p.

Madsen, J.D., P.A. Chambers, W.F. James, E.W. Koch, and D.F. Westlake. 2001. The interaction between water movement, sediment dynamics and submersed macrophytes. Hydrobiologia 44: 71–84. https://doi.org/10.1023/A:1017520800568

Marcus, W. A., Kearney, M.S. 1991. Upland and coastal sediment sources in a Chesapeake Bay Estuary. Annals of the Association of American Geographers. 81(3): 408-424. https://doi.org/10.1111/j.1467-8306.1991.tb01702.x

Merrill, J.Z., Cornwell, J.C. 2002. The role of oligohaline marshes in estuarine nutrient cycling. In: Concepts and Controversies in Tidal Marsh Ecology. Springer, Dordrecht. https://doi.org/10.1007/0-306-47534-0_19

Miller, D., Ladd, J., Nieder, W.C., 2006. Channel morphology in the Hudson River Estuary: Historical changes and opportunities for restoration. In: American Fisheries Society Symposium. American Fisheries Society. p 29.

Minello, T.J., Rozas, L.P., Baker, R. 2012. Geographic variability in salt marsh flooding patterns may affect nursery value for fishery species. Estuaries and Coasts. 35: 501–514. https://doi.org/10.1007/s12237-011-9463-x

Mitsch, W.J., Gosselink, J.G., 2000. Wetlands in the tidal freshwater zone. In: Wetlands: Functioning, Biodiversity Conservation, and Restoration. Springer-Verlag, Berlin. pp 117-148.

Nardin, W., Edmonds, D.A., Fagherazzi, S. 2016. Influence of vegetation on spatial patterns of sediment deposition in deltaic islands during flood. Advances in Water Resources. 93: 236-248. https://doi.org/10.1016/j.advwatres.2016.01.001

Naylor, M. 2003. Water Chestnut (*Trapa natans*) in the Chesapeake Bay Watershed: A Regional Management Plan. Maryland Department of Natural Resources. https://www.fws.gov/anstaskforce/Species%20plans/Water%20Chestnut%20Mgt%20Plan.pdf

NFWF. 2014. National Fish and Wildlife Foundation. 2014 Conservation investments. http://www.nfwf.org/whoweare/mediacenter/Documents/2014-nfwf-grants-list.pdf. Accessed 7 April 2021.

Neubauer, S. C., Anderson, I. C., Constantine, J. A., Kuehl, S. A. 2002. Sediment deposition and accretion in a Mid-Atlantic (U.S.A) Tidal Freshwater Marsh. Estuarine, Coastal, and Shelf Science. 54: 713-727. https://doi.org/10.1006/ecss.2001.0854

Neubauer, S. C. 2008. Contributions of mineral and organic components to tidal freshwater marsh accretion. Estuarine, Coastal and Shelf Science. 78: 78-88. https://doi.org/10.1016/j.ecss.2007.11.011

NOAA. 2014. 2013 USGS Lidar: NY post-Sandy, Ulster, Dutchess, Orange Counties. Charleston, South Carolina: Office for Coastal Management.

NYSIS. 2019. New York State Invasive Species Information, Water Chestnut. http://nyis.info/invasive_species/water-chestnut/

Odum, W.E., 1988. Comparative ecology of tidal freshwater and salt marshes. Annual Review of Ecology and Systematics. 19: 147-176.

Pasternack, G.B. and Brush, G.S. 2001. Seasonal variations in sedimentation and organic content in five plant associations on a Chesapeake Bay tidal freshwater delta. Estuarine, Coastal and Shelf Science. 53: 93-106. https://doi.org/10.1006/ecss.2001.0791

Ralston, D.K., Geyer, W.R., and Lerczak. J.A. 2008. Subtidal salinity and velocity in the Hudson River Estuary: Observations and modeling. Journal of Physical Oceanography. 38: 753–887. https://doi.org/10.1175/2007JPO3808.1

Ralston, D.K., Geyer, W.R. 2009. Episodic and long-term sediment transport capacity in the Hudson River Estuary. Estuaries and Coasts. 32: 1130. https://doi.org/10.1007/s12237-009-9206-4

Ralston, D.K., Talke, S., Geyer, W.R., Al-Zubaidi, H.A., Sommerfield, C.K., 2019. Bigger tides, less flooding: Effects of dredging on barotropic dynamics in a highly modified estuary. Journal of Geophysical Research: Oceans. 124: 196–211. https://doi.org/10.1029/2018JC014313

Ralston, D.K., Yellen, B., Woodruff, J.D. 2021. Watershed suspended sediment supply and potential impacts of dam removals for an estuary. Estuaries and Coasts. https://doi.org/10.1007/s12237-020-00873-3

Reed, D., van Wesenbeeck, B., Herman, P.M., and Meselhe, E. 2018. Tidal flat-wetland systems as flood defenses: Understanding biogeomorphic controls. Estuarine, Coastal and Shelf Science. 213: 269–282. https://doi.org/10.1016/j.ecss.2018.08.017

Schoellhamer, D.H., S.A. Wright, and J.Z. Drexler. 2012. A conceptual model of sedimentation in the Sacramento-San Joaquin Delta. San Francisco Estuary and Watershed Science. 10(3). https://doi.org/10.15447/sfews.2012v10iss3art3

Spencer, T., Schuerch, M., Nicholls, R.J., Hinkel, J., Lincke, D., Vafeidis, A.T., Reef, R., McFadden, L., Brown, S. 2016. Global coastal wetland change under sea-level rise and related stresses: The DIVA Wetland Change Model. Global and Planetary Change. 139: 15–30. https://doi.org/10.1016/j.gloplacha.2015.12.018

Squires, D.F., 1992. Quantifying anthropogenic shoreline modification of the Hudson River and Estuary from European contact to modern time. Coastal Management. 20: 343–354. https://doi.org/10.1080/08920759209362183

Sritrairat, S., Peteet, D.M., Kenna, T.C., Sambrotto, R., Kurdyla, D., Guilderson, T. 2012. A history of vegetation, sediment and nutrient dynamics at Tivoli North Bay, Hudson Estuary, New York. Estuarine, Coastal and Shelf Science. 102–103: 24–35. https://doi.org/10.1016/j.ecss.2012.03.003

Strayer, D.L. 2010. Alien species in fresh waters: ecological effects, interactions with other stressors, and prospects for the future. Freshwater Biology. 55(1): 152-174. https://doi.org/10.1111/j.1365-2427.2009.02380.x

Tabak, N.M., Laba, M., Spector, S. 2016. Simulating the effects of sea level rise on the resilience and migration of tidal wetlands along the Hudson River. PLoS ONE. 11(4): e0152437. https://doi:10.1371/journal.pone.0152437

Temmerman, S., Govers, G., Wartel, S., Meire, P. 2003. Spatial and temporal factors controlling short-term sedimentation in a salt and freshwater tidal marsh, Scheldt Estuary, Belgium, SW Netherlands. Earth Surface Processes and Landforms. 28:739-755. https://doi.org/10.1002/esp.495

US Census Bureau. 2011. Population Distribution and Change: 2000 to 2010. 2010 Census Briefs. https://www.census.gov/prod/cen2010/briefs/c2010br-01.pdf

USGS. 2016. The StreamStats program. Online at http://streamstats.usgs.gov, accessed on May 4, 2020.

Wall, G.R., Nystrom, E.A. and Litten, S. 2008. Suspended sediment transport in the freshwater reach of the Hudson River Estuary in Eastern New York. Estuaries and Coasts. 31: 542–553. https://doi.org/10.1007/s12237-008-9050-y

Wahlen, M. and Lewis, D.M. 1980. Green Lake: Dating of laminated sediment. EOS Trans. Amer. Geophys. Un. Abs. 61/46: 964.

Whigham, D.F., Baldwin, A.H., Barendregt, A. 2009. Tidal freshwater wetlands. In: Coastal wetlands: an integrated ecosystem approach. Elsevier, Amsterdam. pp 515-534.

Work, P.A., Downing-Kunz, M., Drexler, J.Z. 2021. Trapping of suspended sediment by submerged aquatic vegetation in a tidal freshwater region: field observations and long-term trends. Estuaries and Coast. 44: 734-749. https://doi.org/10.1007/s12237-020-00799-w

Yellen, B., Woodruff. J.D., Ladlow, C., Ralston, D.K., Fernald, S., Lau, W. 2020. Rapid tidal marsh development in anthropogenic backwaters. Earth Surf. Process. Landforms. 2021; 1–20. https://doi.org/10.1002/esp.5045